REVIEWS OF GEOPHYSICS AND SPACE PHYSICS, VOL. 10, NO. 3, PP. 761–797, AUGUST 1972

Deformation of the Earth by Surface Loads

W. E. FARRELL

Cooperative Institute for Research in Environmental Sciences
University of Colorado, Boulder, Colorado 80302

and

National Oceanic and Atmospheric Administration
Boulder, Colorado 80302

The static deformation of an elastic half-space by surface pressure is reviewed. A brief mention is made of methods for solving the problem when the medium is plane stratified, but the major emphasis is on the solution for spherical, radially stratified, gravitating earth models. Love-number calculations are outlined, and from the Love numbers, Green's functions are formed for the surface mass-load boundary-value problem. Tables of mass-load Green's functions, computed for realistic earth models, are given, so that the displacements, tilts, accelerations, and strains at the earth's surface caused by any static load can be found by evaluating a convolution integral over the loaded region.

CONTENTS

1. INTRODUCTION

Analysis of the deformation of an elastic solid by surface tractions is a classic problem of current geophysical interest because of recent advances in the study of the tide in the solid earth. Part of this tide is due to the earth's yielding to the body forces exerted by the sun and moon. This aspect of the phenomenon is rather well understood. In addition to the tidal body force, however, surface forces from the pressure of the harmonically varying ocean tide act on the earth, producing 'load tides,' which are difficult to distinguish from the 'body-force' tide. It is difficult to distinguish between these tides because their temporal characters are similar, both ultimately being derived from the same astronomical input. However, the spatial behavior of the two tidal effects is quite different. Whereas the body tide varies smoothly over the earth's surface, the load tide is more irregular because of the discontinuity in the forcing function at the coastline and because the ocean tides form localized circulations around the amphidromes.

The load tide can be separated from the body tide if the earth's response to the tidal body force can be accurately calculated. This is, in fact, possible to a sufficiently high degree of approximation. The various acceptable earth models differ only slightly in their response to the tidal body force, so that simple subtraction of the calculated body tide from the observed tide gives a good estimate of the load tide, provided that local geologic structure and departures from radial symmetry are relatively unimportant. Studies of the gravity tide [*Pertsev,* 1970; *Farrell,* 1970; *Kuo et al.,* 1970; *Prothero and Goodkind,* 1972], the tilt tide [*Blum and Hatzfeld,* 1970; *Lambert,* 1970], and the strain tide [*Berger and Lovberg,* 1970] have established the predominant importance of load tides and have shown that the ocean-load effects can be determined quite accurately, especially near the coastline, where they are typically responsible for about 10% of the gravity tide, 25% of the strain tide, and 90% of the tilt tide. It is therefore possible that these load effects can be used to provide useful information either about the tides in the ocean or, where the ocean tides are well known, about the elastic properties of the earth's crust.

Study of the load tide is considerably more complicated than study of the body tide. The most obvious difference is in the nature of the driving force, which is known to high accuracy for the body tide but to very low accuracy for the load tide. Astronomical observations precisely establish the body force, but the empirical description of the tides in the deep sea is only just beginning [*Munk et al.,* 1970], and their theoretical calculation from the hydrodynamical equations is still far from perfect [*Pekeris and Accad,* 1970]. Besides this contrast in the driv-

ing force, the response to ocean loads depends strongly on the locally variable properties of the crust and mantle, whereas the response to the body force depends more on the earth's over-all properties. The customary idealization of the earth by a model composed of homogeneous, isotropic, spherical layers is much more likely to be valid for the body tide, which has significant displacements through most of the earth's volume, than for the load tide, whose displacements are appreciable only in the crust and upper mantle. Differences in earth structure, for example, beneath ocean basins and continents, will therefore affect the load tide more than the body tide.

There are other sources of surface pressure fluctuations that produce observable geophysical effects. Near the sea, the crust flexes under the pressure of low-frequency ocean waves, this static loading being quite distinct from the resonant loading that generates the higher-frequency, propagating microseisms. The atmosphere, too, produces surface loads from the pressure variations associated with atmospheric tides and weather. It seems that except along coastlines, quasi-static atmospheric loading generates the low-frequency seismic background [*Haubrich*, 1972], so that in principle it is possible to improve earthquake recordings by measuring atmospheric pressure fluctuations and subtracting the calculated load effect.

Stoneley [1926] and *Takeuchi* [1950] made the earliest computations of the tidal deformations of the earth. The surface loading of simple earth models was solved by *Slichter and Caputo* [1960], *Jobert* [1960], and *Caputo* [1961, 1962]. *Kaula* [1963] considered internal mass loading. *Kuo* [1969] used the Thompson-Haskell matrix method to find the response of a layered, nongravitating half-space to surface stresses. The alternative procedure of numerically integrating the equilibrium equations for the layered half-space is developed here in section 2. The much more difficult problem of finding the deformations caused by arbitrary internal stress and displacement singularities has application to the static and dynamic displacements from earthquakes. *Singh* [1970] and *Ben-Menahem et al.* [1970] discuss this subject.

The calculation given here of the deformation by surface mass loads of spherical gravitating earth models closely follows *Longman*'s [1962, 1963] adaptation of the *Pekeris and Jarosch* [1958] and *Alterman et al.* [1959] formulation of the eigenvalue problem for an elastic gravitating sphere. First the Love numbers are calculated for a given earth model, then the proper weighted sums of the Love numbers are totaled to form the various Green's functions. Thus calculation of the load response is reduced to the evaluation of a convolution integral. Of course, if the geophysical load of interest has its energy concentrated in the low-degree spherical harmonics, it may be efficient to evaluate the load effect in the wave-number domain, multiplying the Love numbers by the load expansion coefficients [*Pertsev*, 1966, 1970]. In calculating tidal loading, however, it is better to convolve the cotidal data with the load Green's function. This is because most of the load effect comes from the water closest to the observation site, and to represent this load accurately in a spherical harmonic expansion would require global knowledge of the small-scale variations in the ocean tide. The convolution method makes optimum use of the most accurate and important ocean-tide data, those

pertaining to the immediate vicinity of the geophysical measurement.

There is an alternative to the Love-number method for calculating the earth's response to a surface mass load. *Gilbert* [1970] has called attention to the work of *Rayleigh* [1945, chapter 4] on the response of a harmonic oscillator to an arbitrary input. Rayleigh showed how the response could be expressed as a weighted sum of the eigenfunctions, with the weights depending on the driving force and inversely on the frequency squared of each mode. Assuming the existence of tables of eigenfrequencies and eigenfunctions for a given earth model, this method is probably most useful for calculating the far-field response. The response near the load is mostly governed by upper-mantle structure, which strongly affects only the high-degree modes of the earth.

Only perfectly elastic earth models, driven at frequencies much less than the gravest eigenfrequency, are considered here, and, because we are assuming the earth is perfectly elastic, two important aspects of quasi-static geophysical loading are not covered. These are the frictional dissipation of energy in a lossy (finite Q) elastic solid and the approach to isostasy through viscous flow in the mantle. The first feature is important in tidal loading; the second feature dominates the earth's response to loads that have time scales of millennia (the Pleistocene glaciers).

Seismological studies have established that disturbances faster than 1 cycle per hour decay with a Q of the order of 100–1000, and from observational data the dissipation function $Q^{-1}(r)$ can be found [*Backus and Gilbert*, 1970]. Since $Q^{-1}(r)$ is a function of radius, the earth's response to harmonic (at the several tidal frequencies) surface loads will lag behind the driving force, and the lag will vary with distance from the load, as well as with frequency. The lag could be computed by assuming a $Q^{-1}(r)$ structure and including a dissipation term in the equations of motion. At present, the phases in the tidal load data are much more uncertain than the few degrees attributable to mantle friction, but accurate loading data could potentially justify numerical calculation. Not only does the load tide contribute to lunar tidal friction (the effect is probably quite small), but also loading Q's could be compared with seismic Q's to study the possible variation of Q with frequency. The body-force tide, too, lags its driving force. In this case only a few spherical harmonics are important; hence the eigenmode summation technique [*Gilbert*, 1970] is the appropriate calculation method, assigning to each mode its observed Q [*Lagus and Anderson*, 1968].

Glacial loading causes flow in the mantle, and to describe this phenomenon requires a constitutive relation more complicated than the perfectly elastic equation. One common model is the Maxwell solid, whose behavior is governed by a Newtonian viscosity, as well as the usual density and Lamé parameters [*Cathles*, 1971]. The time dependence in the response is handled by the Fourier or Laplace transform formalism. Green's functions for surface loads on a viscous earth model are found by taking the input to be a δ function in time as well as space, so that two inversions are required to construct Green's functions from the transformed variables. Calculation of the geophysical response to a melting ice sheet then requires the evaluation of both a temporal and a spatial convolution integral; hence the computing effort for glacial loads is much greater than for tidal loads.

2. BOUSSINESQ'S PROBLEM

The archetypal load study is the calculation of the response of a nongravitating, elastic half-space to surface pressure. The Green's functions for this boundary-value problem are associated with the name of *Boussinesq* [1885]. This is an appropriate starting point for several reasons. The method of solution adopted here is exactly that used later in this paper for the spherical, stratified, gravitating earth, and it exhibits all the essential features but none of the algebraic complexity of the spherical calculation. Also, near a point load, the Boussinesq solution is the limiting value of the spherical solution (to the extent that the elastic forces dominate the gravitational forces), and the analytic expressions of the former are a useful check on the numerical calculations of the latter. Furthermore, the Boussinesq problem supplies a standard response, convenient for normalizing the spherical Green's functions.

a. The basic solution. In a homogeneous nongravitating medium, the static displacement vector $\mathbf{s}$ satisfies the elastic equilibrium equation

$$\sigma \nabla \nabla \cdot \mathbf{s} - \mu \nabla \times \nabla \times \mathbf{s} = 0 \tag{1}$$

λ and μ are the Lamé parameters, $\sigma = \lambda + 2\mu$ and $\eta = \lambda + \mu$. Let us define a cylindrical coordinate system with basis vectors $\mathbf{e}_z$, $\mathbf{e}_r$, $\mathbf{e}_\theta$ and let $z \leq 0$ be the volume occupied by the half-space. We seek solutions to (1) under the condition that the free surface be stress free except for a point force at the origin. There is no θ dependence in the solution, since the point force is axially symmetric, hence we let

$$\mathbf{s} = u(z, r)\mathbf{e}_z + v(z, r)\mathbf{e}_r \tag{2}$$

We introduce the Hankel (or Fourier-Bessel) transforms of order 0 and 1 on the r variable [*Watson*, 1966, chapter 14] and let U and V be the components of the transformed displacement:

$$\begin{aligned} u(z, r) &= \int_0^\infty U(z, \xi) J_0(\xi r)\xi \, d\xi \\ v(z, r) &= \int_0^\infty V(z, \xi) J_1(\xi r)\xi \, d\xi \end{aligned} \tag{3}$$

In cylindrical coordinates, the stress-strain relations are

$$\begin{aligned} \tau_{zz} &= \sigma \frac{\partial u}{\partial z} + \frac{\lambda}{r} \frac{\partial (rv)}{\partial r} \\ \tau_{rz} &= \mu \left(\frac{\partial v}{\partial z} + \frac{\partial u}{\partial r} \right) \end{aligned} \tag{4}$$

with transforms $T_{zz}(z, \xi)$, $T_{rz}(z, \xi)$, of order 0 and 1, respectively.

Transforming the equilibrium equation and introducing the stress-strain relations give the first-order system

$$\frac{\partial}{\partial z}\begin{bmatrix} U \\ V \\ T_{zz} \\ T_{rz} \end{bmatrix} = \begin{bmatrix} 0 & -\lambda\xi\sigma^{-1} & \sigma^{-1} & 0 \\ \xi & 0 & 0 & \mu^{-1} \\ 0 & 0 & 0 & -\xi \\ 0 & 4\mu\eta\xi^2\sigma^{-1} & \lambda\xi\sigma^{-1} & 0 \end{bmatrix}\begin{bmatrix} U \\ V \\ T_{zz} \\ T_{rz} \end{bmatrix} \tag{5}$$

When λ and μ are constant, standard methods [*Frazer et al.*, 1965, chapter 5] give for the four linearly independent solutions to (5)

$$\begin{bmatrix} U \\ V \\ T_{zz} \\ T_{rz} \end{bmatrix} = e^{\pm\xi z}\begin{bmatrix} 1 \\ \mp 1 \\ \pm 2\mu\xi \\ -2\mu\xi \end{bmatrix} \tag{6a}$$

and

$$\begin{bmatrix} U \\ V \\ T_{zz} \\ T_{rz} \end{bmatrix} = e^{\pm\xi z}\begin{bmatrix} \mp\xi z + \dfrac{(\lambda + 3\mu)}{\eta} \\ \xi z \\ -2\mu\xi\left(\xi z \mp \dfrac{\sigma}{\eta}\right) \\ \pm 2\mu\xi\left(\xi z \mp \dfrac{\mu}{\eta}\right) \end{bmatrix} \tag{6b}$$

[*McConnell*, 1965, equation 41]. These must now be combined with four multipliers $A_\pm$ and $B_\pm$ so that the boundary conditions are satisfied. For the displacements and stresses to vanish as $z \to -\infty$, $A_- = B_- = 0$. A_+ and B_+ are determined by the two free-surface stress conditions.

At the surface, $\tau_{rz} = 0$. We let τ_{zz} be the stress arising from a unit force acting uniformly over a disk of radius α,

$$\begin{aligned} \tau_{zz}(0, r) &= -\frac{1}{\pi\alpha^2} \qquad r < \alpha \\ \tau_{zz}(0, r) &= 0 \qquad r > \alpha \end{aligned} \tag{7}$$

so that

$$\begin{aligned} T_{zz}(0, \xi) &= -\frac{1}{2\pi}\left[\frac{2J_1(\xi\alpha)}{\xi\alpha}\right] \\ T_{rz}(0, \xi) &= 0 \end{aligned} \tag{8}$$

As $\alpha \to 0$, the disk load reduces to a δ function. In this limit, $2J_1(\xi\alpha)/\xi\alpha \to 1$ and $T_{zz} \to -1/2\pi$, the transform of the δ function in cylindrical coordinates. The bracketed quantity in (8) is thus a disk factor associated with the finite-sized load. We let the disk factor be unity now, but since the final solution depends linearly on τ_{zz}, it is easily reinserted later.

With $z = 0$ in (6), conditions (8) ($\alpha = 0$) suffice to determine A_+ and B_+. Combining the two solutions gives for the transformed variables

$$\begin{bmatrix} U \\ V \end{bmatrix} = -\frac{e^{\xi z}}{4\pi\mu\xi} \begin{bmatrix} \frac{\sigma}{\eta} - \xi z \\ \frac{\mu}{\eta} + \xi z \end{bmatrix} \tag{9}$$

which are inverted (equation 3) to yield the standard solutions for the displacements caused by a unit point force pressing vertically on the surface of an elastic half-space:

$$\begin{aligned} u(z, r) &= -\frac{1}{4\pi\mu R}\left(\frac{\sigma}{\eta} + \frac{z^2}{R^2}\right) \\ v(z, r) &= -\frac{1}{4\pi\eta r}\left(1 + \frac{z}{R} + \frac{\eta r^2 z}{\mu R^3}\right) \end{aligned} \tag{10}$$

where $R^2 = r^2 + z^2$. *Lamb* [1902] derived the Boussinesq solution (equation 10) by inverting (9), but his derivation of (9) was different from the one given here.

b. Disk loads. The disk factor can be put back into (9), but only when $z = 0$ are the inverse transforms readily calculable in terms of standard functions. The unit force acting uniformly across a disk of radius α gives transformed surface displacements

$$\begin{bmatrix} U(0, \xi) \\ V(0, \xi) \end{bmatrix} = -\frac{1}{4\pi\eta\xi} \begin{bmatrix} \frac{2J_1(\xi\alpha)}{\xi\alpha} \end{bmatrix} \begin{bmatrix} \frac{\sigma}{\mu} \\ 1 \end{bmatrix} \tag{11}$$

The inversion integrals (equation 3) [*Gradshteyn and Ryzhik*, 1965, equation 6.574] yield

$$\begin{aligned} u(0, r) &= -\frac{\sigma}{2\pi\mu\eta\alpha} F\left(\tfrac{1}{2}, -\tfrac{1}{2}; 1; \frac{r^2}{\alpha^2}\right) \qquad r < \alpha \\ u(0, r) &= -\frac{\sigma}{4\pi\mu\eta r} F\left(\tfrac{1}{2}, \tfrac{1}{2}; 2; \frac{\alpha^2}{r^2}\right) \qquad r > \alpha \end{aligned} \tag{12}$$

(*Lamb* [1902], but his equation 37 is in error by a factor of $\frac{1}{2}$.)

$$\begin{aligned} v(0, r) &= -\frac{r}{4\pi\eta\alpha^2} \qquad r < \alpha \\ v(0, r) &= -\frac{1}{4\pi\eta r} \qquad r > \alpha \end{aligned} \tag{13}$$

where $F(\alpha, \beta; \gamma; x)$ is the hypergeometric function. These hypergeometric functions are expressible in terms of the complete elliptic integrals

$$\begin{aligned} E(k) &= \int_0^{\pi/2} (1 - k^2 \sin^2 \phi)^{1/2}\, d\phi \\ K(k) &= \int_0^{\pi/2} (1 - k^2 \sin^2 \phi)^{-1/2}\, d\phi \end{aligned} \tag{14}$$

to give alternatively [*Love*, 1929, section 3.8]

$$u(0, r) = -\frac{\sigma}{\pi^2 \mu \eta \alpha} E\left(\frac{r}{\alpha}\right) \qquad r < \alpha$$
$$u(0, r) = -\frac{\sigma r}{\pi^2 \mu \eta \alpha^2}\left[E\left(\frac{\alpha}{r}\right) - \left(1 - \frac{\alpha^2}{r^2}\right)K\left(\frac{\alpha}{r}\right)\right] \qquad r > \alpha \tag{15}$$

Replacing $F(\frac{1}{2}, \frac{1}{2}; 2; \alpha^2/r^2)$ by the leading terms in its power series expansion gives the approximate solution

$$u(0, r) \approx -\frac{\sigma}{4\pi\mu\eta r}\left(1 + \frac{\alpha^2}{8r^2}\right) \qquad r \gg \alpha \tag{16}$$

c. Elliptic loads. The pressure distribution at the edge of the uniform disk load is discontinuous, and this leads to the nonphysical result that the surface tilt at $r = \alpha$ is infinite. The infinity is not present when the pressure smoothly approaches zero at the edge, as is illustrated by the case of parabolic or elliptic loading. Let the applied stress be of the form

$$\tau_{zz}(0, r) = -\frac{3}{2\pi\alpha^2}(1 - r^2/\alpha^2)^{1/2} \qquad r < \alpha$$
$$\tau_{zz}(0, r) = 0 \qquad r > \alpha \tag{17}$$

keeping the total force exerted unity. Using a result in *Watson* [1966, section 12.11] with a change of variable, the transformed stress is

$$T_{zz}(0, \xi) = -\frac{1}{2\pi}\left[\frac{3j_1(\xi\alpha)}{\xi\alpha}\right] \tag{18}$$

The bracketed part of (18) is the factor associated with the elliptic stress distribution; j_1 is the spherical Bessel function. The transformed displacements at the surface are given by (11), substituting the elliptic factor in place of the disk factor. The inversion integrals are again evaluated in terms of the hypergeometric function, giving surface displacements

$$u(0, r) = -\frac{3\sigma}{16\mu\eta\alpha}\left(1 - \frac{r^2}{2\alpha^2}\right) \qquad r < \alpha$$
$$u(0, r) = -\frac{\sigma}{4\pi\mu\eta r} F\left(\tfrac{1}{2}, \tfrac{1}{2}; \tfrac{5}{2}; \frac{\alpha^2}{r^2}\right) \qquad r > \alpha \tag{19}$$

[*Terazawa*, 1916, section 4], and

$$v(0, r) = -\frac{1}{4\pi\eta r}\left[1 - \left(1 - \frac{r^2}{\alpha^2}\right)^{3/2}\right] \qquad r < \alpha$$
$$v(0, r) = -\frac{1}{4\pi\eta r} \qquad r > \alpha \tag{20}$$

Alternatively, the relation

$$F\left(\tfrac{1}{2}, \tfrac{1}{2}; \tfrac{5}{2}; \frac{\alpha^2}{r^2}\right) = \frac{3r}{2\alpha}\left[\left(1 - \frac{r^2}{2\alpha^2}\right)\sin^{-1}\left(\frac{\alpha}{r}\right) + \frac{r}{2\alpha}\left(1 - \frac{\alpha^2}{r^2}\right)^{1/2}\right]$$

can be used for computing the exterior vertical displacement.

d. General results for the areal strain and dilatation. Let $P(r, \theta)$ be an arbitrary distribution of surface pressure acting on a homogeneous, elastic half-space. Then the surface areal strain is

$$(\epsilon_{rr} + \epsilon_{\theta\theta})_{z=0} = -\frac{P}{2\eta}$$

a result that can be established by expressing the strains in terms of the logarithmic and Newtonian potential functions [*Love*, 1929, section 1.1]. Likewise it can be shown that the surface pressure causes a vertical strain

$$(\epsilon_{zz})_{z=0} = -\frac{P}{2\eta}$$

so that the volumetric strain or dilatation at the surface is always

$$(\epsilon_{rr} + \epsilon_{\theta\theta} + \epsilon_{zz})_{z=0} = -\frac{P}{\eta}$$

In the special situation where P vanishes at some point r_o, θ_o, the areal strain and dilatation vanish there also, irrespective of the pressure distribution elsewhere.

e. Gravitational effects. The equation of motion in a homogeneous, self-gravitating medium is considerably more complicated than the purely elastic equation 1. For conventional values of λ, μ, ρ, and ξ, however, the elastic forces dominate the gravitational, and the gravitational potential perturbation in Boussinesq's problem is approximately found by neglecting the elastic-gravitational coupling and solving Poisson's equation

$$\nabla^2\phi = -4\pi G\rho\nabla\cdot\mathbf{s} \tag{21}$$

with the components of $\mathbf{s}$ given by (10). Above the half-space, ϕ satisfies Laplace's equation. Furthermore, the linearized boundary conditions require that ϕ and $(\nabla\phi + 4\pi G\rho\mathbf{s})\cdot\mathbf{e}_z$ be continuous across the plane $z = 0$. If we transform (21) with

$$\phi(z, r) = \int_0^\infty \Phi(z, \xi)J_0(\xi r)\xi\, d\xi \tag{22}$$

and introduce the transformed Boussinesq solution (equation 9), we have

$$\begin{aligned} \left(\frac{\partial^2}{\partial z^2} - \xi^2\right)\Phi(z, \xi) &= \frac{2G\rho}{\eta} e^{\xi z} \qquad z < 0 \\ \left(\frac{\partial^2}{\partial z^2} - \xi^2\right)\Phi(z, \xi) &= 0 \qquad z > 0 \end{aligned} \tag{23}$$

The solution to (23) that satisfies the boundary conditions is

$$\begin{aligned} \Phi(z, \xi) &= \frac{G\rho}{2\mu\xi^2}\left(1 + \frac{2\mu}{\eta}\xi z\right)e^{\xi z} \qquad z \leq 0 \\ \Phi(z, \xi) &= \frac{G\rho}{2\mu\xi^2} e^{-\xi z} \qquad z \geq 0 \end{aligned} \tag{24}$$

The perturbed potential gives an acceleration on the deformed surface of $-\nabla\phi(0^+, r)$, with components a_z^ϕ and a_r^ϕ. In addition to this acceleration arising from the perturbed density field, there are two further components in the total surface acceleration that are geophysically important. If the half-space in Boussinesq's problem is taken for an earth model, the unperturbed density field causes a surface acceleration $-g\mathbf{e}_z$, and this acceleration has vertical gradient $2g/a$. The unit vertical force is then exerted by a point mass $1/g$, with vertical and horizontal accelerations a_z^m and a_r^m. Vertical displacement u gives an acceleration change $a_z^u = 2gu/a$ from the gradient in the unperturbed field. Finally, there is an apparent horizontal acceleration $a_r^u = -g\, du/dr$ arising from the tilt of the deformed surface.

To the first order, $a_z^m = a_r^\phi = 0$. If we take the Boussinesq solution for Φ, differentiate it, and evaluate the inversion integral (equation 22), then

$$a_z^\phi = \frac{G\rho}{2\mu r}$$

If we use (10) to compute a_z^u and let $G = 3g/4\pi\langle\rho\rangle a$ where $\langle\rho\rangle$ and a are the earth's mean density and radius, respectively,

$$\frac{a_z^\phi}{a_z^u} = -\frac{3}{4}\frac{\rho}{\langle\rho\rangle}\left(\frac{\eta}{\sigma}\right) \tag{25}$$

For the horizontal components, again using the Boussinesq solution for u and $1/g$ for the mass load, we get the ratio

$$\frac{a_r^m}{a_r^u} = \frac{3\mu}{ag\langle\rho\rangle}\left(\frac{\eta}{\sigma}\right) \tag{26}$$

(25) and (26) have been derived for the point pressure, but since they are independent of r, they are valid for any surface pressure distribution whatever, so long as the decoupling of the elastic and gravitational potential equations is valid. When the half-space is incompressible ($\lambda = \infty$), $\eta/\sigma = 1$. The incompressible form of (26) is the famous result of *Darwin* [1907]; *Lamb* [1917, equation 6] evaluated the compressibility effect. The incompressible version of (25) corresponds to the classic Bouguer gravity anomaly.

With typical values of the parameters, $a_z^\phi/a_z^u = -0.29$, $a_r^m/a_r^u = 0.175$. Thus the perturbed density field reduces the free-air gravity effect by about a third, and the tilt of the deformed boundary is about six times larger than the tilt caused by the direct attraction of the mass load.

f. The stratified half-space. When λ and μ depend on z, the displacements cannot in general be determined analytically (but see *Jobert* [1960] for a discussion of the case when Poisson's ratio is constant and the rigidity μ varies exponentially with depth) and the Green's functions are found by numerical methods. Finite-difference or finite-element techniques can be applied to the governing partial differential equation directly, obviating the Hankel transforms. The latter method is finding growing application in engineering stress analysis [*Zienkiewicz*, 1971] and has the great advantage that almost any spatial variation in material properties is allowed, including stress-free fault planes. For

plane-layered models, however, the Hankel transform approach presented here is the proper method of solution. Even when the Lamé parameters are arbitrary functions of z, the equilibrium equation can be transformed and reduced to the matrix equation (5). To solve the matrix equation, the medium beneath some starting depth z_o is assumed to be a uniform half-space. The starting solutions at z_o are then given by the two appropriate column vectors in (6), where $\lambda = \lambda(z_o)$ and $\mu = \mu(z_o)$. The depth z_o, which depends inversely on the wave number ξ, is chosen so that the half-space starting solutions make a negligible contribution to the surface solutions. Both starting solutions can then be propagated to the surface by a series of matrix multiplications, in each layer the propagator or layer matrix being formed from the four homogeneous solutions 6 [*Gilbert and Backus*, 1966; *Kuo*, 1969]. Alternatively the matrix differential equation 5 can be numerically integrated from z_o to the surface [*Farrell*, 1970]; this is the preferred technique for solving the spherical earth problem.

Just as for the uniform half-space, the surface boundary conditions determine the transformed solution, which is computed for a range of wave number ξ. The displacement Green's functions are then obtained by calculating numerically the Hankel inversion integrals (3). To obtain the tilt and strain Green's functions it is better not to differentiate the displacements numerically. Rather, there are appropriate Bessel function kernels such that numerical integration can be used to compute the strains and tilts from the transformed displacement integrands. It is desirable to reinsert the disk factor in these integrals for rapid convergence. This method of computation was used by *Farrell* [1970] for evaluating load corrections for a number of tidal gravity observations.

3. MASS LOADS ON THE SPHERICAL EARTH

Only a brief account is given here of the formulation of the spherical earth problem. A more complete discussion is given by *Longman* [1962, 1963], *Takeuchi et al.* [1962], *Kaula* [1963], *Alsop and Kuo* [1964], and, in connection with the earth's free oscillations, by *Pekeris and Jarosch* [1958], *Alterman et al.*, [1959], *Backus* [1967], *Gilbert and Backus* [1968a], and *Wiggins* [1968].

a. Numerical integration of the equations of motion. The equations of motion, Fourier transformed with respect to time, are the linearized equation for the conservation of linear momentum and Poisson's equation

$$\begin{aligned} \nabla\cdot\boldsymbol{\tau} - \nabla(\rho g\mathbf{s}\cdot\mathbf{e}_r) - \rho\nabla\phi + g\nabla\cdot(\rho\mathbf{s})\mathbf{e}_r - \omega^2\rho\mathbf{s} &= 0 \\ \nabla^2\phi = -4\pi G\nabla\cdot(\rho\mathbf{s}) & \end{aligned} \tag{27}$$

[Backus, 1967]. ρ and g are the density and gravitational acceleration in the absence of motion, $\mathbf{s}$ is the displacement vector, $\boldsymbol{\tau}$ is the stress tensor, and ϕ is the perturbation in the ambient gravitational potential ϕ_1 plus the potential of any externally applied gravitational force field ϕ_2. Since the applied force field is created by matter outside the earth, its potential satisfies Laplace's equation within the earth and thus nowhere appears explicitly in the equations of motion. It only enters through the free-surface boundary conditions.

Equations (27), a coupled set of 4 second-order linear differential equations, are to be solved for spherically symmetric earth models whose properties are functions of r alone. At the free surface the tangential stress vanishes; hence the single equation for the toroidal motion drops out, leaving the spheroidal system in the three scalar variables s_r, s_θ, and ϕ. Proceeding in the usual fashion, $\mathbf{s}$ and ϕ are expanded in vector spherical harmonics. Because the surface load is axially symmetric, the solution does not depend on longitude; hence only the particular Legendre order $m = 0$ occurs in the expansions. Thus

$$\begin{aligned} \mathbf{s} &= \sum_{n=0}^{\infty} \left(U_n(r) P_n(\cos\theta)\mathbf{e}_r + V_n(r) \frac{\partial P_n(\cos\theta)}{\partial\theta} \mathbf{e}_\theta \right) \\ \phi &= \sum_{n=0}^{\infty} \Phi_n(r) P_n(\cos\theta) \end{aligned} \tag{28}$$

The stress-strain relations are used to introduce the two stress variables τ_{rr} and $\tau_{r\theta}$, and a third variable, related to the potential gradient, is defined by

$$q = \frac{\partial\phi}{\partial r} + \frac{n+1}{r}\phi + 4\pi G\rho \mathbf{s}\cdot\mathbf{e}_r$$

With $T_{rr,n}$, $T_{r\theta,n}$, and Q_n, the transforms of τ_{rr}, $\tau_{r\theta}$, and q, transforming (27) leads to the matrix equation

$$\frac{d\mathbf{Y}}{dr} = \mathbf{A}\mathbf{Y} \tag{29}$$

where $\mathbf{Y} = (U_n, V_n, T_{rr,n}, T_{r\theta,n}, \Phi_n, Q_n)^t$ and t denotes transposition. (By analogy with the flat-earth vocabulary, I say 'transformed variables' for $U_n(r)$, etc. rather than the more clumsy 'radial coefficients in the spherical harmonic expansions.') $\mathbf{A}$ is a 6×6 coefficient matrix depending on ω, r, n and λ, μ, ρ. Equation 29 is analogous to equation 5 and if $\rho = 0$ and r and n are large, $\mathbf{A}$ reduces to the matrix written there.

In the fluid core, $\mu = 0$ and equation 29 becomes a fourth-order system, since the tangential displacement and $\tau_{r\theta}$ can be eliminated. A further simplification follows if $\omega = 0$, for then the Adams-Williamson condition holds, and (29) reduces to a second-order system involving only Φ and Q [*Longman*, 1963]. In this work I have solved the normal-mode equation, with ω the frequency of the semidiurnal tide. The choice of core model is not important, however, because the fluid core only affects the low-degree Love numbers. Within the earth the displacements caused by a surface load decrease as $(r/a)^n$, and above degree $n = 10$ the core can be totally ignored. In neither formulation of the core equations are the earth's rotation and the existence of internal gravity-wave modes taken into account, but these effects seem important only for the particular tidal frequency K_1 [*Jeffreys and Vicente*, 1957; *Molodensky*, 1961].

In the case of a uniform sphere, where λ, μ, and ρ are constant, there are analytic expressions for the elements of the three (in a fluid, two) linearly independent $\mathbf{Y}$ that are finite at $r = 0$. The calculation of these vectors $\mathbf{Y}$ is not as simple as the solution of equation (5), but the method is outlined in *Pekeris and Jarosch* [1958] and *Gilbert and Backus* [1968*a*] (see also *Wiggins* [1968]). The

solutions involve ordinary (and in some cases modified) spherical Bessel functions and powers of r.

For computation, suitable nondimensional variables are introduced. The numerical integration of (29) for a stratified earth model is begun at some radius r_o, below which it is assumed that λ, μ, and ρ are constant. r_o is determined by the desired accuracy of the solution. The solutions for a homogeneous sphere of radius r_o are taken as starting values for $\mathbf{Y}$. The Runge-Kutta-Gill scheme [*Shanks*, 1966], with variable step size [*Gilbert and Backus*, 1968*b*], was used in the numerical integration. The final solution is the mix of the three linearly independent solutions that satisfies the three free-surface boundary conditions.

b. Surface boundary conditions. The Boussinesq boundary condition was that a unit (massless) force press down at the origin. The boundary conditions on the transformed variables were found by transforming a disk-shaped force and taking the limit as the disk radius vanished. The same procedure is followed here, except that the surface force is applied by a mass γ and the presence of gravitational effects requires a third boundary condition on the potential gradient variable q. The potential variable ϕ in the equations of motion 27 has two components, ϕ_1 and ϕ_2, where ϕ_1 is the potential of the earth's distorted density field and ϕ_2 is the potential of the applied mass load. The linearized boundary conditions are that ϕ_1, ϕ_2, and $(\nabla\phi_1 + 4\pi G\rho\mathbf{s})\cdot\mathbf{e}_r$ be continuous across $r = a$, that $\nabla\phi_2\cdot\mathbf{e}_r$ change by $4\pi G\gamma$, and that $\tau_{rr}(a) = -g\gamma$ and $\tau_{r\theta}(a) = 0$.

Let γ be a unit mass distributed uniformly across a disk of radius α. Expanding γ in a Legendre series [*Hobson*, 1955; *Longman*, 1963] gives

$$\gamma = \sum_{n=0}^{\infty} \Gamma_n P_n(\cos\theta)$$

$$\Gamma_n = [P_{n-1}(\cos\alpha) - P_{n+1}(\cos\alpha)]/[4\pi a^2(1 - \cos\alpha)] \qquad n > 0$$

$$\Gamma_0 = 1/4\pi a^2$$

but with $z = \cos\alpha$

$$P_{n-1}(z) - P_{n+1}(z) = \frac{2n+1}{n(n+1)}(1 - z^2)\frac{\partial P_n(z)}{\partial z}$$

so that

$$\Gamma_n = \frac{2n+1}{4\pi a^2}\left[-\frac{(1+\cos\alpha)}{n(n+1)\sin\alpha}\frac{\partial P_n(\cos\alpha)}{\partial\alpha}\right] \qquad n > 0 \tag{30}$$

The first quantity in (30) is the Legendre expansion of the δ function in spherical coordinates; the bracketed part is again a disk factor associated with the finite-sized distribution. With α small and n large,

$$-\frac{(1+\cos\alpha)}{n(n+1)\sin\alpha}\frac{\partial P_n(\cos\alpha)}{\partial\alpha} \to \frac{2J_1(n\alpha)}{n\alpha}$$

the cylindrical form of the disk factor, and thus approaches one in the limit. The transformed surface potential of the point mass load is

$$\Phi_{2,n} = \frac{4\pi Ga}{2n+1}\Gamma_n = \frac{ag}{m_e} \tag{31}$$

where m_e is the mass of the earth. By using (30) and (31), the transformed boundary conditions are then

$$T_{rr,n}(a) = -g\Gamma_n$$
$$T_{r\theta,n}(a) = 0$$
$$Q_n(a) = -4\pi G\Gamma_n$$

The transformed mass distribution (30) enters linearly into the transformed surface boundary conditions, and hence it linearly affects the transformed solution vector. Thus, when numerically solving (29), with no loss of generality, γ can be assumed to be a δ function with the disk factor set equal to unity. With this condition, U_n, V_n, and Φ_n are determined for the point mass load.

c. Loads of degree 0 and 1. The special cases $n = 0, 1$ are handled differently from the higher-degree terms. A load of P_0 form is uniform over the whole earth and causes radial displacement (because the earth is compressible) but neither tangential displacement nor potential perturbation. The differential equation 29, when $n = 0$, is a second-order system involving U and T_{rr}, and as its solution I have used the result $U_0(a) = -0.134\ a/m_e$ calculated by *Longman* [1963] for a point mass load on the Gutenberg earth model having an Adams-Williamson core ($\omega = 0$). The ocean tide, of course, conserves mass, so that the $n = 0$ coefficient in the spherical harmonic expansion of the tidal elevation vanishes; hence there is no $n = 0$ load effect. The U_0 term must be included in the Green's function, however, even though it contributes nothing to the tidal load when the convolution extends over all the world ocean.

It has commonly been thought that displacements of degree 1 are impossible since they shift the center of mass of the earth, but *Cathles* [1971] has observed that this is incorrect in the surface-mass-load problem. What is true is that the center of mass of earth plus load is fixed in space, but there is no constraint on the earth alone. The melting of the Canadian and Fennoscandian ice sheets 10,000 years ago and the tide in the ocean both furnish examples of surface loads containing $n = 1$ terms, and hence having their center of mass not coincident with the center of mass of the earth. Thus, as a load of this form changes position (we are concerned just with redistributed surface loads, not loads with net changes in the total mass), there is a proportional shift of the center of mass of the earth in space. The earth is also strained by the load, but several changes from the usual scheme are required to calculate the response.

In the earth's mantle, there are three linearly independent solutions to (29) that we discard because they are infinite at $r = 0$, and there are three solutions that we propagate from the bottom of the mantle to the surface, there mixing them to match the three free-surface boundary conditions. In the special case $n = 1$, when $\omega = 0$ the three starting solutions to (29) can be linearly combined to give one vector of the form

$$\mathbf{Y}^s = (1, 1, 0, 0, -g, 0)^t$$

where the superscript s indicates that this vector represents a rigid shift of the earth (note there are no stresses). The vector $\mathbf{Y}^s$ also is a solution in the core when

$n = 1$. Regardless of mantle structure,

$$\frac{d\mathbf{Y}^s}{dr} = \mathbf{A}\mathbf{Y}^s = 0$$

so that the numerical integration of (29) propagates $\mathbf{Y}^s$ to the surface unaltered. But this implies that the 3×3 matrix (with elements T_{rr}, $T_{r\theta}$, Q for each solution), which must be inverted to find the weight multiplying each solution, is singular, since it can be put into the form where one column is identically zero. Expressed differently, when $n = 1$ and $\omega = 0$, of the three valid solutions to (29), one is a shift of the origin. This has homogeneous boundary values in the stress and potential gradient variables; thus we are left with only two vectors that must satisfy three boundary conditions. For a valid solution to exist, a consistency relation

$$T_{rr} + 2T_{r\theta} + \frac{g}{4\pi G} Q = 0$$

must hold. In a homogeneous sphere with $\omega = 0$ and $n = 1$ this relation can be proved analytically for all solutions, and its validity in a layered earth for small ω has been shown numerically.

Computationally one proceeds as follows. Rather than rearrange the three conventional mantle starting solutions into two solutions plus a rigid shift, any two solutions are chosen and propagated from the core to the surface. At the surface the correct mix of the two solutions is found by satisfying any two of the three boundary conditions. The consistency relation assures us that the third boundary condition is met automatically.

The response to a P_1 type load has now been found, but only to within an arbitrary shift of the origin, since any amount of the vector $\mathbf{Y}^s$ can be added to the solution without altering the boundary values. There are two possible choices for the origin: the center of mass of earth plus load or the center of mass of the undeformed earth. The latter is the more logical choice of origin, since the strains associated with a rigid translation of the whole earth are not observable to an earth-based observer without reference to an inertial coordinate system. To have the origin located at the center of mass of the undeformed earth, it is necessary that the center of mass of the deformed matter vanish. This is accomplished by adding the proper amount of $\mathbf{Y}^s$ to the numerically calculated solution. If superscript c denotes the solution vector calculated as described above, the correct solution is

$$\mathbf{Y} = \mathbf{Y}^c + \alpha\mathbf{Y}^s$$

and α is found by setting the center of mass of the $\mathbf{Y}$ vector equal to zero.

Consider the exterior potential ϕ_1 expressed as an infinite series in the moments of the perturbed mass distribution. The $n = 1$ surface mass load causes just a first-degree term in the exterior potential; thus, if z is the shift in the center of mass along the $\theta = 0$ direction,

$$\phi_1 = -\frac{Gm_e z}{r^2} \cos\theta$$

and

$$\Phi_1 = -\frac{Gm_e z}{r^2}$$

if we write Φ_1 for $\Phi_{1,1}$. The displacement of the center of mass for the $n = 1$ load is thus

$$z = -\frac{\Phi_1(a)a^2}{Gm_e}$$

But $\Phi_1(a) = \Phi_1^c(a) - \alpha g$ so that for $z = 0$, $\alpha = \Phi_1^c(a)/g$ and $\mathbf{Y} = \mathbf{Y}^c + \Phi_1^c(a)\mathbf{Y}^e/g$. Expressed in terms of the Love numbers, we get the simple result $h_1 = h_1^c + k_1^e$, $l_1 = l_1^c + k_1^e$, and $k_1 = 0$. Typical values are $h_1 = -0.290$, $l_1 = 0.113$.

4. LOVE NUMBERS

a. General comments. It is conventional to discuss the static deformation of an elastic sphere in terms of the dimensionless Love numbers h_n, l_n, and k_n, each of which in fact is a function of the two variables n and r. When displacements U_n, V_n, and $\Phi_{1,n}$ arise from an axially symmetric force field with transformed potential $\Phi_{2,n}$,

$$\begin{bmatrix} U_n(r) \\ V_n(r) \\ \Phi_{1,n}(r) \end{bmatrix} = \Phi_{2,n}(r) \begin{bmatrix} \frac{h_n(r)}{g} \\ \frac{l_n(r)}{g} \\ k_n(r) \end{bmatrix} \tag{32}$$

defines the Love numbers. Equation 31 gives $\Phi_{2,n}(a)$ for the point mass load. We are primarily interested in the displacements at the surface, and, when the radial argument is not explicitly indicated, the value $r = a$ is to be taken.

The Love numbers are intimately related to the transformed Green's functions, and, just as any differential equation has a distinct Green's function for each set of boundary conditions, so the system (27) has a different triplet of Love numbers (functions) for different boundary conditions.

Two sorts of force fields (hence boundary conditions) are of interest. One is the tidal force of the moon and sun, and the other is the force of a surface mass load. The only difference in the associated boundary conditions is that on the free surface the latter exerts a normal stress that is missing in the former. *Munk and MacDonald* [1960] distinguished the mass-load Love numbers by a superscript prime. *Longman* [1963] calls them load-deformation coefficients. I shall call both types simply Love numbers because in practice there is seldom confusion.

b. The flat-earth approximation. The Boussinesq problem yielded the displacements and potential perturbation generated by a point force pressing on the surface of an elastic half-space. These were the three Green's functions. The Green's functions for the loading of a homogeneous elastic sphere, in the limit of decreasing distance θ from the load, reduce to the Boussinesq solution, and it is

not surprising that there are asymptotic expressions for the Love numbers in terms of the material properties λ, μ, and ρ. We find these expressions by relating (28) to (3) and (22).

When θ is small, it is the terms with n large that dominate the spherical harmonic expansion of the response. Under these conditions, the Legendre functions can be replaced by the Bessel function approximations

$$\begin{aligned} P_n(\cos\theta) &\to J_0[(n+\tfrac{1}{2})\theta] \\ \frac{\partial P_n(\cos\theta)}{\partial\theta} &\to -(n+\tfrac{1}{2})J_1[(n+\tfrac{1}{2})\theta] \end{aligned} \tag{33}$$

and the sums in (28) are then asymptotically equivalent to the integrals

$$\begin{aligned} \mathbf{s} &= \int_0^\infty \left\{\frac{ah_n}{m_e} J_0[(n+\tfrac{1}{2})\theta]\mathbf{e}_r - \frac{al_n}{m_e}(n+\tfrac{1}{2})J_1[(n+\tfrac{1}{2})\theta]\mathbf{e}_\theta\right\} dn \\ \phi_1 &= \int_0^\infty \frac{agk_n}{m_e} J_0[(n+\tfrac{1}{2})\theta]\, dn \end{aligned} \tag{34}$$

where U_n, V_n, and $\Phi_{1,n}$ have been written in terms of the point mass potential $\Phi_{2,n}$ and the Love numbers, and $r = a$.

The $\mathbf{e}_z$, $\mathbf{e}_r$, $\mathbf{e}_\theta$ cylindrical coordinate system used in Boussinesq's problem has the plane $z = 0$ tangent to the sphere of the $\mathbf{e}_r$, $\mathbf{e}_\theta$, $\mathbf{e}_\lambda$ spherical system at $\theta = 0$, $r = a$. Coordinate distance θ in the spherical system becomes r/a in the cylindrical system and wave number $\xi = (n+\frac{1}{2})/a$, with $dn = a\, d\xi$.

A point mass in Boussinesq's problem gives transformed surface displacements

$$\begin{aligned} U &= -\frac{g\sigma}{4\pi\mu\eta\xi} \\ V &= -\frac{g}{4\pi\eta\xi} \\ \Phi &= \frac{3\rho g^2}{8\pi\langle\rho\rangle a\mu\xi^2} \end{aligned} \tag{35}$$

(Because gravitational forces were neglected in Boussinesq's problem, $\Phi_2 = 0$ and this $\Phi(0, \xi)$ is the same as $\Phi_{1,n}(a)$ in the spherical self-gravitating case.)

The equivalence between the asymptotic spherical solution (34) and the exact half-space solution, found by substituting (35) into (3) and (22), gives the relations

$$\begin{bmatrix} h_n \\ nl_n \\ nk_n \end{bmatrix} = \frac{gm_e}{4\pi a^2\eta} \begin{bmatrix} -\dfrac{\sigma}{\mu} \\ 1 \\ -\dfrac{3\rho\eta}{2\langle\rho\rangle\mu} \end{bmatrix} \tag{36}$$

correct to the order of $1/n$. Close enough to the point load, a layered earth model responds in the same way as a homogeneous sphere that has the properties of the

topmost layer. Thus, at large n, numerically computed Love numbers can be checked against the analytic expressions (36).

5. GREEN'S FUNCTIONS

Calculating the Love numbers for an earth model is only half the solution of the point-load problem. Corresponding to the Hankel inversion integrals of the flat-earth case, the proper weighted sums of the Love numbers must be totaled to form the Green's functions. The Green's functions depend both on r and on θ, but we are only interested in their dependence on angular distance θ at the earth's surface $r = a$. The general techniques presented here are still applicable to computing the response at interior points, except that the interior rather than the surface values of the Love numbers would be used. The interior Love numbers, although not tabulated here, come automatically from the numerical solution of the equations of motion.

The Green's functions are the two displacement components and the gravitational potential perturbation caused by the point surface mass load. Geophysically we are more interested in knowing the vertical and horizontal acceleration, the tilt, and the strain tensor, since these are the observable effects of the loading. We shall call the point response functions for these derivative variables Green's functions also, though they are not true Green's functions in the strict mathematical sense.

Love-number calculations are standard, but there has been just one previous attempt to form the surface-load Green's functions [*Longman*, 1963]. Longman was not particularly successful (he only found some of the far-field responses) for two reasons. First, Love numbers were only calculated up to degree $n = 40$; I have gone as high as $n = 10{,}000$. Second, some of the series converge slowly, and there are better methods than the one Longman used to evaluate the infinite sums.

The six Green's functions form three natural groups: (1) the horizontal and vertical displacements, (2) the horizontal and vertical accelerations, and (3) the strain-tensor elements. All the calculations are similar, but only the vertical displacement is given detailed discussion. The other five responses are covered more briefly.

a. Displacements. The surface vertical displacement at distance θ from the point mass load is

$$u(\theta) = \frac{a}{m_e} \sum_{n=0}^{\infty} h_n P_n(\cos \theta) \tag{37}$$

from the definitions of h_n, equation 32, and the surface potential of the point mass (31).

If n is large enough, h_n, nl_n, and nk_n become constant, and I define

$$\lim_{n \to \infty} \begin{bmatrix} h_n \\ nl_n \\ nk_n \end{bmatrix} = \begin{bmatrix} h_\infty \\ l_\infty \\ k_\infty \end{bmatrix} \tag{38}$$

Approximate expressions for these limits, derived from the Boussinesq problem, are written in equations 36, but as the exact values we take those computed for the largest n. The approach to the limit, and the differences between the approximate and computed limits, are clearly shown in the Love-number plot, Figure 1, and in Table A2.

Using the asymptotic value for h_n, (37) can be written

$$u(\theta) = \frac{ah_\infty}{m_e} \sum_{n=0}^{\infty} P_n(\cos\theta) + \frac{a}{m_e} \sum_{n=0}^{\infty} (h_n - h_\infty) P_n(\cos\theta) \tag{39}$$

The first sum is known exactly. The second sum terminates after a finite number of terms, since $(h_n - h_\infty)$ is zero above $n = N$, the maximum Legendre degree. This artifice is sometimes called Kummer's transformation. With the expression for the first sum given in Appendix 1, equation 39 becomes

$$u(\theta) = \frac{ah_\infty}{2m_e \sin(\theta/2)} + \frac{a}{m_e} \sum_{n=0}^{N} (h_n - h_\infty) P_n(\cos\theta) \tag{40}$$

The finite sum in (40), although better behaved than the infinite sum in (37), still converges rather slowly because the amplitude of P_n falls off only as $n^{-1/2}$ (equation 42). Two further devices are now applied to speed the convergence. The first operation is to put the disk factor back into the transformed potential; the second is to use Euler's transformation on the series.

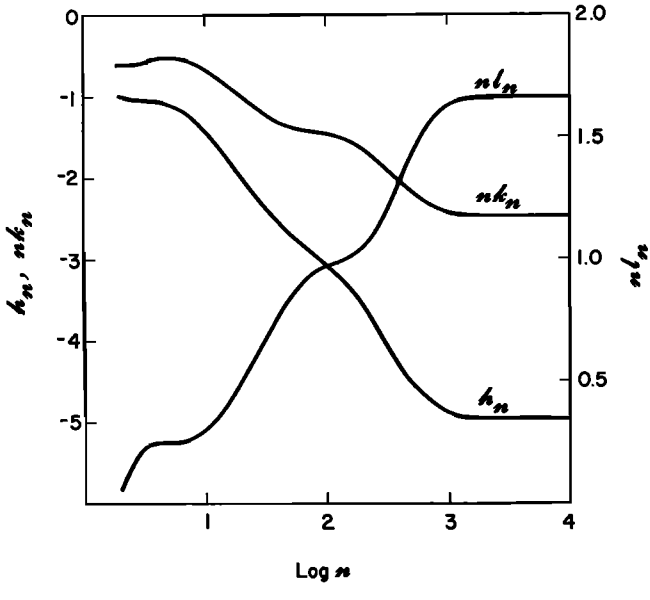

Fig. 1. Love numbers for a unit mass load on the surface of a Gutenberg-Bullen A earth model. Selected values are listed in Table A2. At $n = 10{,}000$, the computed Love numbers agree with the Boussinesq approximation to within 1%. The Love numbers for the other earth models differ significantly from these Love numbers above $n = 20$ to 30.

The exact nature of the surface mass load was immaterial for the Love-number calculation; the δ-function source was merely convenient. For the Green's functions, however, it is correct to use only the δ-function load with coefficients ag/m_e (at $r = a$) (equation 31). The disk load approaches a δ function as the disk radius α approaches zero, keeping the total mass unity. Thus the sum in (40) is equivalent to

$$\lim_{\alpha \to 0} \frac{a}{m_e} \sum_{n=0}^{N} (h_n - h_\infty) \left[\frac{-(1 + \cos \alpha)}{n(n + 1) \sin \alpha} \frac{\partial P_n(\cos \alpha)}{\partial \alpha} \right] P_n(\cos \theta) \tag{41}$$

The point in inserting the bracketed disk factor is that it provides an additional $n^{-3/2}$ decay in the summand. The faster decay is not essential here, but is important for evaluating the tilt and strain sums.

The actual response of the earth model to disk loads could be found by including the disk factor in the infinite sum, the first part of (39), as well as the finite sum (41). For the Green's function, however, the limit $\alpha \to 0$ is taken. One method of finding the limit would be to evaluate (41) for several α and then to apply Aitken's δ^2 process [*Hildebrand,* 1956, p. 445] or some other extrapolation method to the successive approximations. More simply, satisfactory results are obtained merely by setting θ/α large. Values between 10 and 30 still retain the convergence advantage of larger disks but have α small enough that the difference between the point and the disk is negligible. The uniform half-space response to a disk load differs from the point-load response by terms of the order of α^2/r^2 and smaller (equation 16).

The Euler transformation [*Hildebrand,* 1956, chapter 5.9] is a familiar method for rapidly summing an alternating series. The power of the technique lies in the fact that, although the terms in the original series may decrease only slowly with n, the terms in the transformed (and also alternating) series show a decrease of the order of 2^{-n}. There is an elegant algorithm by van Wijngaarden (Appendix 2) that facilitates the numerical application of Euler's transformation. *Dahlquist et al.* [1965] have given a modern discussion of Euler's transformation as well as other somewhat better transformations for speeding the convergence of series.

To apply the Euler transformation, (40) must be written as an alternating series. When n is large,

$$P_n(\cos \theta) \approx \left(\frac{2}{\pi n \sin \theta} \right)^{1/2} \cos \left[(n + \tfrac{1}{2})\theta - \frac{\pi}{4} \right] \tag{42}$$

and for, all n in the range $(4i - 3)\pi/4\theta < n < (4i + 1)\pi/4\theta$, we see that $P_n(\cos \theta)$ is positive (negative) when i is odd (even). Grouping the terms in (40) we can write the sum as

$$\frac{a}{m_e} \sum_{i=0}^{M} a_i(\theta) \qquad M = N\theta/\pi \tag{43}$$

where

$$a_i(\theta) = \sum_{n=j(i)}^{k(i)} (h_n - h_\infty) P_n(\cos \theta) \tag{44}$$

with $j(0) = 0$, $k(0) = \langle \pi/4\theta \rangle$, $j(i) = k(i-1) + 1$, and $k(i) = j(i) + \langle \pi/\theta \rangle$ (the symbol $\langle\ \rangle$ indicates the nearest integer is to be taken). The partial sums (44) are evaluated directly, giving terms $a_i(\theta)$, which alternate in sign (in the limit) so that Euler's transformation can now be applied to (43). When the disk factor is included in the partial sums, $a_i(\theta)$ no longer strictly alternates in sign, but neither this nor the rounding of π/θ to the nearest integer causes any difficulty in practice.

The successive terms in the Euler transformed series involve higher and higher order differences of the terms in the original series. However, the differencing operation is not numerically stable because the relative error in the terms grows as the order of the difference increases. With an analytic summand, round-off errors determine the accuracy of the differences. In this case involving numerically defined functions, the Love numbers, the errors can be much larger, depending on the precision with which the differential equation 29 is integrated. No differencing problems occurred when the Love numbers were calculated to an accuracy of 0.01%.

When θ is small, a large number of terms must be evaluated in (44). (The number of terms in (43) required for accurate summation varies little for $0.01° < \theta < 180°$, 10 terms being typical.) But, when n is large and θ is small, both h_n and P_n are slowly varying functions of n. Thus, for $n > 1000$, the Legendre function in (44) can be replaced by its Bessel function approximation (33) and the Euler-Maclaurin summation formula [*Hildebrand,* 1956, chapter 5.8] can be used to approximate the sum by an integral. Simpson's rule is used to evaluate the integral, the net gain being that only a few of the original summands need to be calculated.

The Love numbers must be known over a large range of Legendre degree n, typically $0 \leq n \leq 10{,}000$. It is not necessary to integrate numerically the equations of motion for each integral n, but instead interpolation can be used on a sparser table of the Love numbers. The spacing in degree between successive h_n, l_n, and k_n can be a rapidly increasing function of n, as can be seen from Figure 1.

The horizontal displacement at the surface is given by

$$v(\theta) = \frac{a}{m_e} \sum_{n=1}^{\infty} l_n \frac{\partial P_n(\cos\theta)}{\partial \theta}$$

Again, if we extract the asymptotic part involving l_∞, we have

$$v(\theta) = \frac{a l_\infty}{m_e} \sum_{n=1}^{\infty} \frac{1}{n} \frac{\partial P_n(\cos\theta)}{\partial \theta} + \frac{a}{m_e} \sum_{n=1}^{\infty} (n l_n - l_\infty) \frac{1}{n} \frac{\partial P_n(\cos\theta)}{\partial \theta} \tag{45}$$

The first sum in (45) is known exactly (Appendix 1), and the second sum is evaluated in the same way as the vertical displacement sum discussed previously.

b. Accelerations: tilt and gravity effects. The difference between g, the acceleration of gravity at the earth's surface, and the acceleration on the deformed boundary after application of the mass load we call $g(\theta)$, the gravitational effect of the load. The deflection of the local vertical, $t(\theta)$, is called the tilt effect. The direct attraction of the mass load is important in both the tilt and gravity changes, and there are also horizontal and vertical accelerations from the per-

turbed density field, proportional to the Love number k_n. The third contribution to the tilt is the slope of the deformed boundary; to gravity it is the change in acceleration from moving through the gradient in the unperturbed gravity field. Both these effects are proportional to the Love number h_n. Combining all three terms and using the point mass potential (31) give the expressions [*Longman*, 1963]

$$g(\theta) = \frac{g}{m_e} \sum_{n=0}^{\infty} [n + 2h_n - (n + 1)k_n]P_n(\cos \theta) \tag{46}$$

$$t(\theta) = -\frac{1}{m_e} \sum_{n=0}^{\infty} [1 + k_n - h_n] \frac{\partial P_n(\cos \theta)}{\partial \theta} \tag{47}$$

In (46) accelerations are positive upward. The first term in each bracket is the direct, or Newtonian, acceleration g^N, t^N, and it is summed exactly (Appendix 1) to give in the two cases

$$g^N(\theta) = -\frac{g}{4m_e \sin (\theta/2)} \tag{48}$$

$$t^N(\theta) = \frac{\cos (\theta/2)}{4m_e \sin^2 (\theta/2)} \tag{49}$$

$g^E = g - g^N$ and $t^E = t - t^N$ are called the 'elastic' accelerations because they arise from the earth's elastic deformation. If the earth were perfectly rigid, the elastic accelerations would vanish. The infinite series for the elastic accelerations are summed in the same way as the vertical displacement.

c. Strain tensor. With u and v being the radial and tangential displacements at the surface, the four nonzero elements of the strain tensor are

$$\begin{aligned} \epsilon_{rr} &= \frac{\partial u}{\partial r} \\ 2\epsilon_{r\theta} &= \frac{1}{a}\frac{\partial u}{\partial \theta} + \frac{\partial v}{\partial r} - \frac{v}{a} \\ \epsilon_{\theta\theta} &= \frac{1}{a}\frac{\partial v}{\partial \theta} + \frac{u}{a} \\ \epsilon_{\lambda\lambda} &= \frac{u}{a} + \cot \theta \frac{v}{a} \end{aligned} \tag{50}$$

The transformed equation of motion gives the relations (see, for instance, *Longman* [1963, equation 18]

$$\begin{aligned} \frac{\partial U_n(r)}{\partial r} &= -\frac{2\lambda}{\sigma r} U_n(r) + \frac{\lambda n(n + 1)}{\sigma r} V_n(r) + \frac{1}{\sigma} T_{rr,n}(r) \\ \frac{\partial V_n(r)}{\partial r} &= -\frac{1}{r} U_n(r) + \frac{1}{r} V_n(r) + \frac{1}{\mu} T_{r\theta,n}(r) \end{aligned} \tag{51}$$

and

$$\frac{\partial u}{\partial r} = \sum_{n=0}^{\infty} \frac{\partial U_n(a)}{\partial r} P_n(\cos\theta)$$
$$\frac{\partial v}{\partial r} = \sum_{n=0}^{\infty} \frac{\partial V_n(a)}{\partial r} \frac{\partial P_n(\cos\theta)}{\partial \theta} \tag{52}$$

At the free surface, $\tau_{r\theta} = 0$, and τ_{rr} is a δ function, so that the two stress terms vanish when (51) is substituted into (52). Introducing the Love numbers, we have for the two radial derivatives at the surface

$$\frac{\partial u}{\partial r} = -\frac{2\lambda}{\sigma a} u + \frac{\lambda}{\sigma m_e} \sum_{n=0}^{\infty} n(n+1) l_n P_n(\cos\theta) \tag{53}$$

$$\frac{\partial v}{\partial r} = -\frac{1}{m_e} \sum_{n=0}^{\infty} h_n \frac{\partial P_n(\cos\theta)}{\partial \theta} + \frac{v}{a} \tag{54}$$

where the surface values of λ and σ are taken. Equations (54) and (50) show that $\epsilon_{r\theta} = 0$ and the strain tensor at the surface is diagonal in the $\mathbf{e}_r$, $\mathbf{e}_\theta$, $\mathbf{e}_\lambda$ spherical coordinate system. Furthermore, $\epsilon_{\lambda\lambda}$ is a simple combination of the displacement components and requires no new computations. Strain element ϵ_{rr} is given by (53) and

$$\epsilon_{\theta\theta} = \frac{u}{a} + \frac{1}{m_e} \sum_{n=0}^{\infty} l_n \frac{\partial^2 P_n(\cos\theta)}{\partial \theta^2} \tag{55}$$

The numerical sums in (53) and (55) are evaluated in the manner discussed previously.

There is a convenient way of checking some of the strain and displacement sums. On the stress-free boundary, the fact that $\tau_{rr}(\theta) = 0$ for $\theta > 0$ implies that

$$\epsilon_{rr} = -\frac{\lambda(a)}{\sigma(a)} (\epsilon_{\theta\theta} + \epsilon_{\lambda\lambda}) \tag{56}$$

for all $\theta > 0$. Therefore, in addition to the direct computation (53), ϵ_{rr} can be computed from the surface areal strain, and the Lamé parameters of the top layer of the earth model. Agreement between the two calculations checks the Green's functions for v, ϵ_{rr}, and $\epsilon_{\theta\theta}$.

6. COMPUTATIONAL RESULTS

Green's functions have been calculated for the Gutenberg-Bullen A earth model (tabulated in *Alterman et al.* [1961]). To explore the influence of the earth's upper mantle, two additional models, formed by replacing the top 1000 km of the G-B earth by the oceanic and continental shield structures of *Harkrider* [1970], were also considered. Conventional Love numbers, $n = 2, 3, 4$, are listed in Table A1 for all three models. Table A2 gives selected values of the load Love numbers for the G-B model as well as the Boussinesq approximations at infinite wave number. The approach to the limit is shown in the plot of the G-B Love numbers, Figure 1. Tabulations of the Green's functions for all three models are

given in Tables A3, A4, and A5. Only the elastic parts of the gravity anomaly g^E and the tilt t^E are listed, and the other two components of the surface-strain tensor are also omitted because they are calculable from $\epsilon_{\theta\theta}$ and the two displacement components (equations 50 and 56).

a. Displacements. Normalized displacements for the G-B model are plotted in Figure 2. The normalizing functions

$$u^*(\theta) = -\frac{g\sigma}{4\pi\mu\eta(a\theta)} = \frac{Gh_\infty}{g(a\theta)}$$

$$v^*(\theta) = -\frac{g}{4\pi\eta(a\theta)} = -\frac{Gl_\infty}{g(a\theta)}$$

are taken from the Boussinesq problem, except that the computed rather than the approximate values of h_∞ and l_∞ are used. Thus Figure 2 plots u/u^* and v/v^*. This normalization removes the basic r^{-1} dependence that characterizes the Green's functions of a uniform half-space, and as $\theta \to 0$, the normalized responses tend to 1.

The distant response is governed by the low-degree Love numbers. To exhibit this relationship, Table 1 shows, for various distances, the maximum Legendre degree N required to evaluate the vertical displacement sum (37). These figures are typical of all the sums.

The influence of the $n = 0$, 1 Love numbers on the distant response is surprisingly large, more so than a glance at Table A2 might indicate. This is

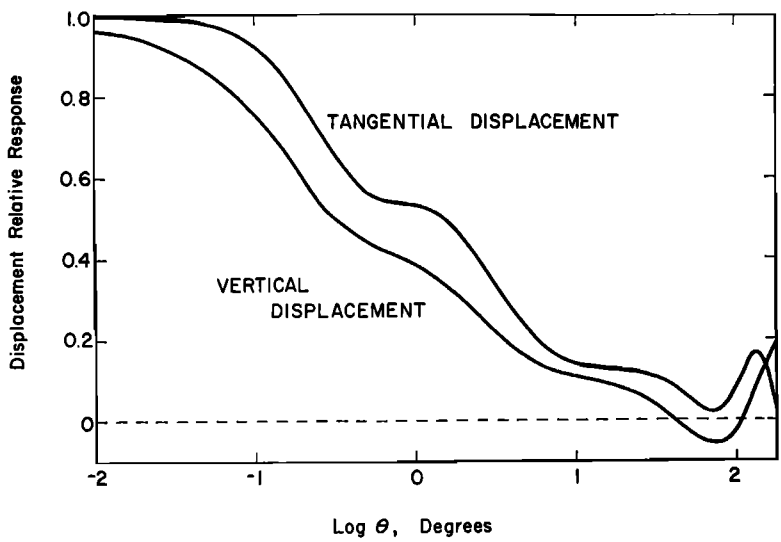

Fig. 2. Surface displacement Green's functions, Gutenberg-Bullen A earth model. The displacements are normalized with respect to the response of a half-space with $v_p = 6.14$ km/sec, $v_s = 3.55$ km/sec or equivalently $h_\infty = -4.96$, $l_\infty = 1.66$. These are the parameters of the top layer of the G-B earth model, and, as $\theta \to 0$, both normalized displacements approach 1. The displacements for the other earth models differ significantly from these for $\theta < 1°$ (Tables A3, A4, and A5).

TABLE 1. The Maximum Degree N Needed to Evaluate the Vertical Displacement at Distance θ from the Point Load

	$\theta = 180°$	$\theta = 130°$	$\theta = 90°$	$\theta = 40°$	$\theta = 20°$
N	11	15	20	60	100

because the sums in (37) and (45), when θ is greater than 90°, are not much larger than a typical term which is of the order of 1 and $\frac{1}{4}$, respectively, in the two cases (Table A2). With only 10 to 20 terms entering into the sum (Table 1), ignoring the $n = 0, 1$ Love numbers radically changes the Green's function for $90° \leq \theta \leq 180°$.

b. Accelerations. The gravity anomaly (vertical acceleration) and tilt Green's functions for the oceanic and continental-shield earth models are plotted in Figures 3 and 4. The responses here are normalized with respect to the direct attractions of the mass load, equations 48 and 49.

The vertical acceleration when θ is small is approximately found by replacing h_n by h_∞ and $(n + 1)k_n$ by k_∞ in (46) and evaluating the two Legendre sums (equations A1 and A2). This gives

$$g(\theta) = \frac{g}{4m_e \sin(\theta/2)} [-1 + 4h_\infty - 2k_\infty]$$

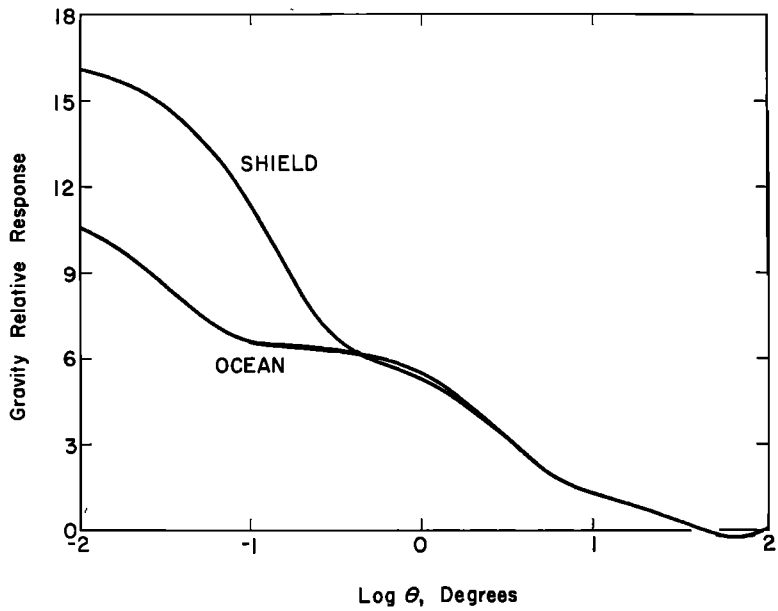

Fig. 3. Elastic part of the vertical acceleration Green's function. Responses normalized with respect to the vertical component of the Newtonian acceleration of the mass load. As $\theta \to 0$, the normalized accelerations tend to 11.9 and 16.7 for the oceanic and shield responses, respectively.

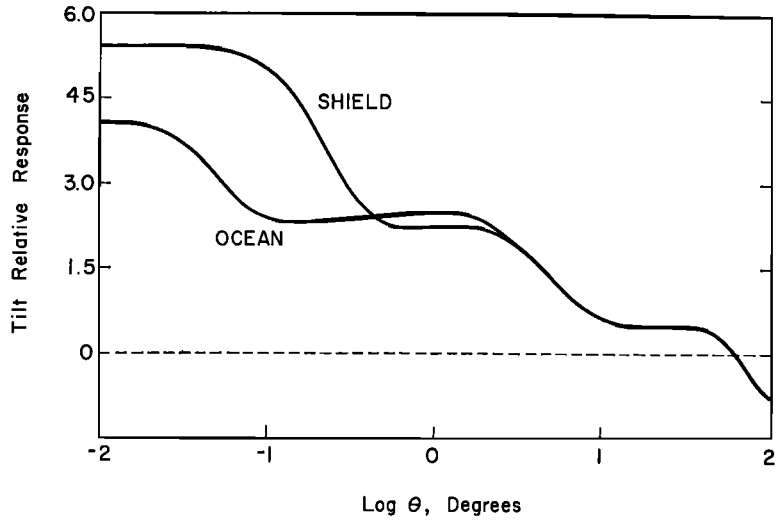

Fig. 4. Elastic part of the tilt Green's function, including the horizontal acceleration of the perturbed density field. Response normalized with respect to the horizontal component of the Newtonian acceleration of the mass load. As $\theta \to 0$, the normalized elastic tilts tend to 4.10 and 5.12 for the oceanic and shield responses, respectively.

showing that near the load the ratio of the potential perturbation effect to the displacement effect is $-k_\infty/2h_\infty$. This ratio can also be calculated from equations 25 and 36. Moreover, Table A2 shows that when $n \geq 3$, $nk_n/2h_n \approx k_\infty/2h_\infty$, etc., so that at all distances the h part and the k part of the acceleration contribute in about this same ratio, even though the total response is far from the small θ limit.

When $\theta \to 0$, the elastic part of the normalized gravity response, g^E/g^N, approaches $2k_\infty - 4h_\infty$.

At near and intermediate distances, the Love number h_n governs the elastic tilt; the horizontal acceleration from the perturbed density field is much less important. Thus the elastic tilt in this range is principally just the slope of the deformed surface. The ratio of the h_n to k_n contributions to the tilt is $-100{:}1$ for $\theta = 1°$, $-10{:}1$ for $\theta = 10°$, and $-3{:}1$ for $\theta = 30°$. As $\theta \to 0$, t^E/t^N approaches $-h_\infty$, from (47) or (26) and (36).

c. Strains. A suitable normalizing function for the strain-tensor components is the derivative of the Boussinesq tangential displacement $\partial v/\partial r$ (equation 10) evaluated on the surface of the half-space

$$\epsilon^* = \frac{g}{4\pi\eta(a\theta)^2} = \frac{Gl_\infty}{g(a\theta)^2}$$

Figure 5 plots $\epsilon_{\theta\theta}/\epsilon^*$ for both mantle models; Figure 6 shows the normalized areal strain, $(\epsilon_{\theta\theta} + \epsilon_{\lambda\lambda})/\epsilon^*$. The surface areal strain vanishes in Boussinesq's problem, and for this reason areal rather than linear strain has sometimes been used in

earth-tide studies to eliminate the ocean-load perturbation. For these models, the procedure is moderately effective at eliminating load effects within 10°.

The displacement components listed in Tables A3, A4, and A5 are used in equation 50 to construct the $\epsilon_{\lambda\lambda}$ Green's function for each earth model. To form the ϵ_{rr} Green's function, equation 56 is used, and the appropriate elastic constant, $\lambda(a)/\sigma(a)$, is given in the footnote to each table.

7. CONCLUSIONS

The immediate application of this work is to the study of ocean tidal loading. There are several lines of attack, which fall into two broad categories: oceanographic studies, and geophysical studies.

The oceanographic problem is, of course, the investigation of the tides in the sea through their loading effect. For example, the Bermuda Island M_2 gravity-tide observation of *Harrison et al.* [1963] shows unambiguously the Atlantic Ocean load tide [*Farrell*, 1970, Figure 1.1]. The load tide at Bermuda is a weighted average of the complex tidal amplitude around the island. The weighting function in this case is just the surface-mass-load gravitational-perturbation Green's function, plotted for two earth models in Figure 3. This Green's function is azimuthally symmetric; hence the load-tide observation provides a moment of the Atlantic Ocean tide, averaged around small circles centered on the observa-

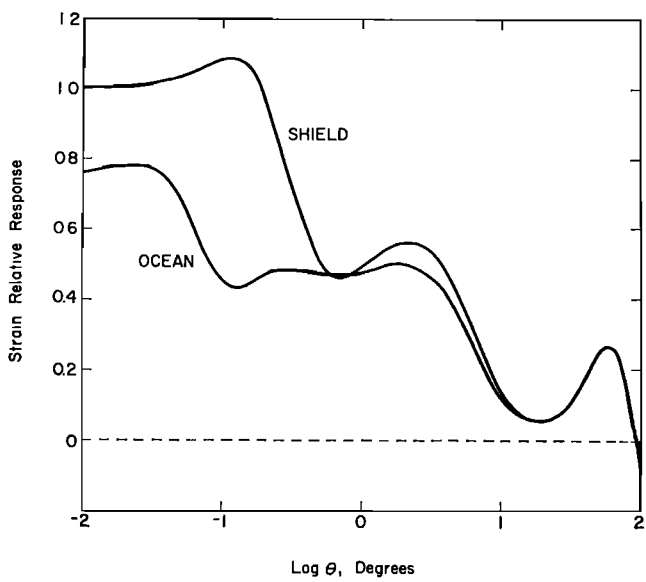

Fig. 5. Linear-strain Green's function $\epsilon_{\theta\theta}$, normalized to the response of a half-space, with $v_p = 6.1$ km/sec, $v_s = 3.54$ km/sec, or, equivalently, $l_x = 1.83$. These are the parameters of the top layer of the continental-shield model; hence normalized shield strain approaches 1 as $\theta \to 0$. Normalized ocean strain, as $\theta \to 0$, approaches (ocean l_x/(shield l_x) = 0.747.

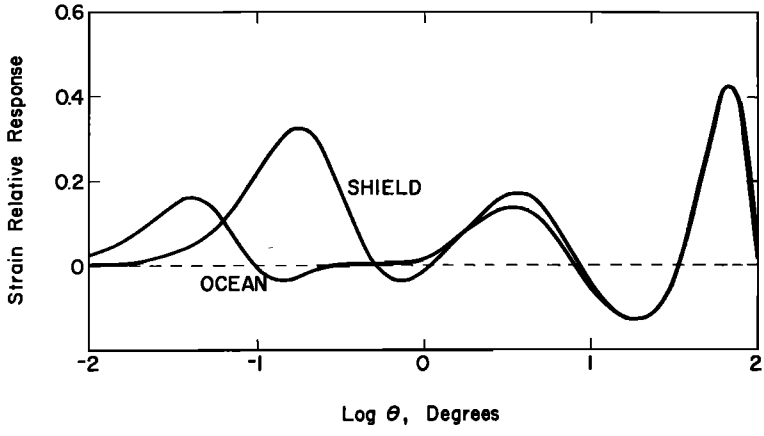

Fig. 6. Areal-strain Green's function, normalized to the linear strain on a half-space, with $v_p = 6.1$ km/sec and $v_s = 3.54$ km/sec or, equivalently, $l_x = 1.83$.

tion site. Other moments of the tides around Bermuda could be found from tilt and strain measurements on the island. The appropriate weighting functions are plotted in Figures 4, 5, and 6, but now, since these are vector and tensor quantities, respectively, the azimuthal averages are different from the gravity average. Different moments of the tide in the Atlantic could be found from further load observations on other Atlantic islands and around the coastlines. These data would be erroneous because of the small effects from distant seas, but, with only general knowledge of the tide elsewhere, the correction for the remote loads can be made sufficiently accurately.

Consider the two-dimensional complex function T, the M_2 tide in the Atlantic. We want to infer T, given a suite of its moments (load observations with various instruments at several sites). If T^o is a first approximation of T, and if T^o is linearly close to T, then the techniques of *Backus and Gilbert* [1970] can be applied to compute from the moments uncertain spatial averages of T, $\langle T \rangle$, where the average at each point is characterized by some known resolving length and accuracy. *Backus and Gilbert* [1970] show how the resolving length and accuracy are related.

This would be an ambitious project and require a wealth of high-quality data. Inversion theory has previously been used to study several one-dimensional functions (for example, the earth's density $\rho(r)$ as a function of radius); here T is a complex function in two dimensions, so that the computational effort is much greater. Eventually it will be more economical just to measure the water elevation directly with instruments like the self-contained capsules of *Snodgrass* [1968]. Nevertheless, load studies can be used in a less rigorous fashion to extrapolate the sparse deep-sea tide data, to verify the numerical tide calculations of *Pekeris and Accad* [1970] and of Hendershott [*Hendershott and Munk*, 1970], and to select 'best' models of the tide in the oceans.

In the oceanographic problem, one assumes that the Green's functions are more accurately known than the configuration of the tidal waters, and, by using

the known Green's functions, one attempts to infer the ocean tide from measurements of the load tide. There are two exceptional areas, the Bay of Fundy and the Irish Sea, where the semidiurnal tide is unusually large and better known than the local earth structure. In these areas, tidal loading is used to study earth structure [*Lambert*, 1970]. Again, the raw data need to be corrected for more distant loads, and the Green's functions given here are suitable for that purpose.

At midcontinent the load tide is a small but unknown perturbation to the body tide. This limits the accuracy with which the astronomically driven body tide can be measured. Given rough models of the ocean tide, the load effects can be removed accurately enough that experimental error becomes the greatest uncertainty in measuring the body tide. More accurate knowledge of phase of the body tide would give information on the earth's dissipation function $Q^{-1}(r)$ at frequencies 10 and 20 times lower than the gravest normal-mode frequency.

APPENDIX 1: LEGENDRE SUMS

Certain infinite sums that arise when the asymptotic values of the Love numbers are separated from the numerical sums are given below. There are analogous formulas for the flat-earth case involving integrals of Bessel functions. The first three sums, given in *Hobson* [1955, chapter 7], are quoted by *Longman* [1963]. One way to establish (A4) is to differentiate the sum over n of $P_n(\cos\theta)/n$ [*Gradshteyn and Ryzhik*, 1965, equation 8.926-1]. The Legendre recurrence relations yield (A5) in terms of (A1), (A2), and (A4). (A1), (A3), and (A5) appear to diverge, but the sums can be established by a suitable limiting process. (A1) and (A3) are proportional to the vertical and horizontal accelerations caused by a point mass on the surface of a sphere, and the trigonometric expressions are easily verified from the gravitational potential function. *Singh and Ben-Menahem* [1968] have given related sums of Legendre series.

$$\sum_{n=0}^{\infty} nP_n(\cos\theta) = -\frac{1}{4\sin(\theta/2)} \tag{A1}$$

$$\sum_{n=0}^{\infty} P_n(\cos\theta) = \frac{1}{2\sin(\theta/2)} \tag{A2}$$

$$\sum_{n=1}^{\infty} \frac{\partial P_n(\cos\theta)}{\partial\theta} = -\frac{\cos(\theta/2)}{4\sin^2(\theta/2)} \tag{A3}$$

$$\sum_{n=1}^{\infty} \frac{1}{n}\frac{\partial P_n(\cos\theta)}{\partial\theta} = -\frac{\cos(\theta/2)[1+2\sin(\theta/2)]}{2\sin(\theta/2)[1+\sin(\theta/2)]} \tag{A4}$$

$$\sum_{n=2}^{\infty} \frac{1}{n}\frac{\partial^2 P_n(\cos\theta)}{\partial\theta^2} = \frac{1+\sin(\theta/2)+\sin^2(\theta/2)}{4\sin^2(\theta/2)[1+\sin(\theta/2)]} \tag{A5}$$

APPENDIX 2: VAN WIJNGAARDEN'S ALGORITHM FOR THE EULER TRANSFORMATION

Let $(-)^n a_n$ be an alternating series with sum S:

$$S = \sum_{n=0}^{\infty} (-)^n a_n \tag{A6}$$

Then it can be shown [*Hildebrand*, 1956] that

$$S = \tfrac{1}{2} \sum_{n=0}^{\infty} \left(-\frac{\Delta}{2}\right)^n a_0$$

where Δ is the forward difference operator. This is the Euler transformation. It is usual to compute S by summing l terms of (A6) and applying Euler's transformation to the remainder. Assume that m terms in the transformed remainder give an accurate enough approximation to S. We absorb the sign into each term, writing $b_n = (-)^n a_n$, and introduce the forward mean operator

$$My_s = \tfrac{1}{2}(y_s + y_{s+1})$$

Then the l, m partial sum can be written

$$S_{l,m} = \sum_{n=0}^{l-1} b_n + \tfrac{1}{2} \sum_{n=0}^{m} M^n b_l$$

$S_{0,0} = \frac{1}{2}b_0$ is the first approximation to S. Next $\frac{1}{2}Mb_0$ is computed and compared with $\frac{1}{2}b_1$. If $\frac{1}{2}Mb_0$ is less than $\frac{1}{2}b_1$, the second approximation is

$$S_{0,1} = S_{0,0} + \tfrac{1}{2}Mb_0$$

If $\frac{1}{2}Mb_0$ is not less than $\frac{1}{2}b_1$,

$$S_{1,0} = S_{0,0} + Mb_0$$

is taken. To advance from the l, m step we take either

$$S_{l,m+1} = S_{l,m} + \tfrac{1}{2}M^{m+1}b_l$$

or

$$S_{l+1,m} = S_{l,m} + M^{m+1}b_l$$

depending on whether $M^{m+1}b_l$ is smaller or larger than $M^m b_{l+1}$. The process is continued until the difference between two successive partial sums is sufficiently small [*National Physical Laboratory*, 1961, p. 124].

APPENDIX 3: NUMERICAL TABLES

TABLE A1. Love Numbers, Stress-Free Surface

	n	h_n	l_n	k_n
G-B earth model	2	0.6114	0.0832	0.3040
		0.6149	0.0840	0.3055
		0.6169	0.0842	0.3062
Oceanic mantle	3	0.2891	0.0145	0.0942
		0.2913	0.0145	0.0943
		0.2923	0.0147	0.0946
Shield mantle	4	0.1749	0.0103	0.0429
		0.1761	0.0103	0.0424
		0.1771	0.0104	0.0427

TABLE A2. Love Numbers, Loaded Surface, G-B Earth Model

n	$-h_n$	nl_n	$-nk_n$
1	0.290	0.113	0
2	1.001	0.059	0.615
3	1.052	0 223	0.585
4	1.053	0.247	0 528
5	1.088	0.243	0 516
6	1.147	0.245	0.535
8	1.291	0 269	0.604
10	1.433	0.303	0.682
18	1.893	0.452	0.952
32	2.379	0 680	1.240
56	2.753	0.878	1.402
100	3.058	0.973	1.461
180	3 474	1.023	1.591
325	4.107	1.212	1.928
550	4.629	1.460	2.249
1,000	4.906	1.623	2.431
1,800	4.953	1.656	2 465
3,000	4.954	1.657	2.468
10,000	4.956	1.657	2 469
∞*	5.005	1.673	2 482

* Boussinesq approximation, equations 36.

TABLE A3. Mass-Loading Green's Functions, G-B Earth Model
(Applied load, 1 kg.)

θ, deg	Radial Displacement, $\times 10^{12}(a\theta)$	Tangential Displacement, $\times 10^{12}(a\theta)$	g^E, $\times 10^{18}(a\theta)$	t^E, $\times 10^{12}(a\theta)^2$	$\epsilon_{\theta\theta}$, $\times 10^{12}(a\theta)^2$
0.0001	−33.64	−11.25	−77.87	33.64	11.248
0.0010	−33.56	−11.25	−77.69	33.64	11.248
0.0100	−32.75	−11.24	−75.92	33.64	11.253
0.0200	−31.86	−11.21	−73.96	33.62	11.278
0.0300	−30.98	−11.16	−72.02	33.58	11.322
0.0400	−30.12	−11.09	−70.11	33.52	11.382
0.0600	−28.44	−10.90	−66.40	33.30	11.537
0.0800	−26.87	−10.65	−62.90	32.92	11.709
0.1000	−25.41	−10.36	−59.64	32.35	11.866
0.1600	−21.80	−9.368	−51.47	29.82	11.988
0.2000	−20.02	−8.723	−47.33	27.78	11.714
0.2500	−18.36	−8.024	−43.36	25.29	11.083
0.3000	−17.18	−7.467	−40 44	23 09	10.303
0.4000	−15.71	−6.725	−36 61	19.84	8.779
0.5000	−14.91	−6.333	−34.32	17.85	7.538
0.6000	−14.41	−6.150	−32.78	16.81	6.682
0.8000	−13.69	−6.050	−30.59	16.25	6.019
1.0	−13.01	−5.997	−28.75	16.32	6.170
1.2	−12.31	−5.881	−27.03	16.33	6.535
1.6	−10.95	−5.475	−23.96	15.86	7.071

TABLE A3. (continued)

θ, deg	Radial Displacement, $\times 10^{12}(a\theta)$	Tangential Displacement, $\times 10^{12}(a\theta)$	g^E, $\times 10^{13}(a\theta)$	t^E, $\times 10^{12}(a\theta)^2$	$\epsilon_{\theta\theta}$, $\times 10^{12}(a\theta)^2$
2.0	−9.757	−4.981	−21.38	14 95	7.114
2.5	−8.519	−4.388	−18.74	13.68	6.830
3.0	−7.533	−3.868	−16.64	12.38	6.332
4.0	−6.131	−3.068	−13.59	10.09	5.261
5.0	−5.237	−2.523	−11.55	8.27	4.297
6.0	−4.660	−2.156	−10.16	6.90	3.445
7.0	−4.272	−1.915	−9.169	5.94	2.765
8.0	−3.999	−1.754	−8.425	5.23	2.230
9.0	−3.798	−1.649	−7.848	4.72	1.800
10.0	−3.640	−1.582	−7.379	4.38	1.485
12.0	−3.392	−1.504	−6.638	3.93	1.122
16.0	−2.999	−1.435	−5.566	3.52	0.788
20.0	−2.619	−1.386	−4.725	3.36	0.712
25.0	−2.103	−1.312	−3.804	3.31	0.812
30.0	−1.530	−1.211	−2.951	3.29	1.104
40 0	−0.292	−0.926	−1.427	2.94	2.040
50.0	0.848	−0.592	−0.279	1.94	2.928
60.0	1.676	−0.326	0.379	0.39	3.253
70.0	2.083	−0.223	0.557	−1.25	2.829
80.0	2.057	−0.310	0.353	−2.71	1.789
90.0	1.643	−0.555	−0.110	−3.76	0.395
100.0	0.920	−0.894	−0.713	−4.31	−1.094
110.0	−0.025	−1.247	−1.357	−4.39	−2.475
120.0	−1.112	−1.537	−1.980	−4.18	−3.656
130.0	−2.261	−1.706	−2.557	−3.72	−4.638
140.0	−3.405	−1.713	−3.076	−3.12	−5.473
150.0	−4.476	−1.540	−3.530	−2.44	−6.191
160.0	−5.414	−1.182	−3.918	−1.67	−6.825
170.0	−6.161	−0.657	−4.243	−0.83	−7.441
180.0	−6 663	0	−4.514	0	−8.203

mks units throughout. The normalizations (a = earth's radius, 6.371×10^6 m, θ = distance from load in radians) are convenient scalings that facilitate intercomparisons. For this model, $\lambda(a)/\sigma(a) = 0.3311$.

TABLE A4. Mass-Loading Green's Functions, Oceanic Mantle Model on G-B Nucleus (Applied load, 1 kg.)

θ, deg	Radial Displacement, $\times 10^{12}(a\theta)$	Tangential Displacement, $\times 10^{12}(a\theta)$	g^E, $\times 10^{13}(a\theta)$	t^E, $\times 10^{12}(a\theta)^2$	$\epsilon_{\theta\theta}$, $\times 10^{12}(a\theta)^2$
0.0001	−27.80	−9.273	−61.88	27.82	9.272
0.0010	−27.52	−9.272	−61.30	27.82	9.273
0.0100	−24.82	−9.091	−55.66	27.70	9.397
0.0200	−22.15	−8.598	−49.99	26.96	9.636
0.0300	−20.04	−7.937	−45.44	25.40	9.639

TABLE A4. (continued)

θ, deg	Radial Displacement, $\times 10^{12}(a\theta)$	Tangential Displacement, $\times 10^{12}(a\theta)$	g^E, $\times 10^{13}(a\theta)$	t^E, $\times 10^{12}(a\theta)^2$	$\epsilon_{\theta\theta}$, $\times 10^{12}(a\theta)^2$
0.0400	−18.53	−7.262	−42.06	23.27	9 234
0.0600	−16.84	−6 257	−37.94	19.10	7.707
0.0800	−16.13	−5.817	−35.92	16 65	6.345
0.1000	−15.87	−5.726	−34.95	15.79	5.690
0.1600	−15.93	−5.876	−34.33	15.94	5.529
0.2000	−15.90	−5 916	−34.07	16.08	5.802
0.2500	−15.83	−5.909	−33.81	16.14	5.941
0.3000	−15.75	−5.884	−33.58	16 25	5.964
0.4000	−15.53	−5.827	−33.10	16 40	5 944
0.5000	−15.27	−5.780	−32.58	16.59	5.862
0.6000	−14.98	−5.738	−32.00	16 71	5 791
0.8000	−14.32	−5.647	−30 71	16.93	5.871
1.0	−13 60	−5.531	−29.31	17.00	5.876
1.2	−12.87	−5.385	−27.88	17.00	5 987
1.6	−11.48	−5.032	−25.11	16.49	6.208
2.0	−10.24	−4.651	−22.60	15 69	6.203
2.5	−8.933	−4.188	−19.88	14 50	6.027
3.0	−7.853	−3.759	−17.60	13 24	5 808
4.0	−6.274	−3.031	−14.15	10.81	5.120
5.0	−5.263	−2.486	−11.82	8.71	4.315
6 0	−4.623	−2.106	−10.24	7.10	3 491
7.0	−4.212	−1.854	−9.153	5.94	2 750
8.0	−3.937	−1.692	−8.365	5.14	2.164
9 0	−3.740	−1.590	−7.766	4.61	1.722
10.0	−3.590	−1.526	−7.289	4 24	1.398
12.0	−3.360	−1.461	−6.558	3.80	0.997
16.0	−2.991	−1.418	−5.520	3.44	0.694
20.0	−2.622	−1.386	−4.704	3.34	0 668
25.0	−2.107	−1.320	−3.792	3.32	0.826
30.0	−1.529	−1.217	−2.943	3.30	1.143
40.0	−0.287	−0.923	−1.436	2.94	2.061
50.0	0.853	−0.584	−0.304	1.91	2.922
60.0	1.676	−0.321	0.336	0 35	3.223
70.0	2.075	−0.224	0.495	−1.29	2.759
80.0	2 040	−0.319	0.275	−2.72	1.709
90.0	1.620	−0.573	−0.194	−3 74	0.312
100.0	0.893	−0.917	−0.794	−4.28	−1.150
110.0	−0.056	−1.273	−1.436	−4.41	−2.549
120.0	−1.144	−1.567	−2.059	−4.10	−3.696
130.0	−2.296	−1.737	−2.636	−3.69	−4.694
140.0	−3.439	−1.742	−3.149	−3.05	−5.473
150.0	−4.509	−1.562	−3.598	−2.38	−6.129
160.0	−5.448	−1.196	−3.987	−1.66	−6.753
170.0	−6.197	−0.663	−4.319	−0.89	−7.431
180.0	−6.702	0	−4.597	0	−8.246

mks units throughout. The normalizations (a = earth's radius, 6.371×10^6 m, θ = distance from load in radians) are convenient scalings that facilitate intercomparisons. For this model, $\lambda(a)/\sigma(a) = 0.3336$.

TABLE A5. Mass-Loading Green's Functions, Continental-Shield Mantle on G-B Nucleus (Applied load, 1 kg.)

θ, deg	Radial Displacement, $\times 10^{12}(a\theta)$	Tangential Displacement, $\times 10^{12}(a\theta)$	g^E, $\times 10^{18}(a\theta)$	t^E, $\times 10^{12}(a\theta)^2$	$\epsilon_{\theta\theta}$, $\times 10^{12}(a\theta)^2$
0.0001	−36.78	−12.39	−87.31	36.79	12.392
0.0010	−36.66	−12.39	−87.02	36.79	12.392
0.0100	−35.41	−12.37	−84.13	36.78	12.406
0.0200	−34.03	−12.31	−80.95	36.75	12.460
0.0300	−32.68	−12.22	−77.81	36.68	12.548
0.0400	−31.36	−12.08	−74.75	36.55	12.666
0.0600	−28.85	−11.72	−68.89	36.07	12.948
0.0800	−26.54	−11.26	−63.49	35.24	13.228
0.1000	−24.49	−10.73	−58.65	34.07	13.427
0.1600	−19.88	−9.092	−47.56	29.24	13.115
0.2000	−17.93	−8.168	−42.69	25.86	12.208
0.2500	−16.37	−7.309	−38.64	22.28	10.738
0.3000	−15.43	−6.746	−36.08	19.67	9.303
0.4000	−14.50	−6.202	−33.26	16.79	7.289
0.5000	−14.07	−6.038	−31.79	15.60	6.247
0.6000	−13.80	−6.014	−30.80	15.16	5.844
0.8000	−13.32	−6.045	−29.29	15.10	5.769
1.0	−12.82	−6.030	−27.95	15.27	6.057
1.2	−12.29	−5.947	−26.66	15.36	6.360
1.6	−11.20	−5.642	−24.22	15.23	6.765
2.0	−10.16	−5.259	−21.99	14.86	6.908
2.5	−8.988	−4.751	−19.53	14.06	6.872
3.0	−7.983	−4.261	−17.42	13.09	6.687
4.0	−6.448	−3.414	−14.16	10.97	5.944
5.0	−5.421	−2.771	−11.90	9.01	5.011
6.0	−4.744	−2.316	−10.33	7.45	4.087
7.0	−4.293	−2.003	−9.219	6.25	3.261
8.0	−3.986	−1.795	−8.410	5.39	2.574
9.0	−3.765	−1.659	−7.792	4.80	2.063
10.0	−3.599	−1.568	−7.305	4.35	1.681
12.0	−3.356	−1.470	−6.569	3.81	1.147
16.0	−2.987	−1.411	−5.537	3.41	0.691
20.0	−2.621	−1.387	−4.723	3.32	0.646
25.0	−2.109	−1.332	−3.806	3.31	0.785
30.0	−1.531	−1.237	−2.950	3.31	1.120
40.0	−0.282	−0.950	−1.418	2.96	2.089
50.0	0.867	−0.609	−0.268	1.92	2.980
60.0	1.698	−0.341	0.389	0.37	3.302
70.0	2.102	−0.239	0.555	−1.29	2.841
80.0	2.069	−0.330	0.341	−2.74	1.792
90.0	1.651	−0.579	−0.122	−3.77	0.394
100.0	0.923	−0.921	−0.719	−4.30	−1.075
110.0	−0.026	−1.277	−1.357	−4.42	−2.493
120.0	−1.118	−1.570	−1.975	−4.14	−3.644
130.0	−2.272	−1.741	−2.548	−3.71	−4.646
140.0	−3.420	−1.748	−3.059	−3.10	−5.427
150.0	−4.495	−1.568	−3.505	−2.42	−6.082
160.0	−5.437	−1.200	−3.893	−1.70	−6.697

TABLE A5. (continued)

θ, deg	Radial Displacement, $\times 10^{12}(a\theta)$	Tangential Displacement, $\times 10^{12}(a\theta)$	g^E, $\times 10^{18}(a\theta)$	t^E, $\times 10^{12}(a\theta)^2$	$\theta_{\theta\theta}$, $\times 10^{12}(a\theta)^2$
170.0	−6.188	−0 665	−4.222	−0.91	−7.362
180.0	−6.693	0	−4.491	0	−8.162

mks units throughout. The normalizations (a = earth's radius, 6.371 × 10^6 m, θ = distance from load in radians) are convenient scalings that facilitate intercomparisons. For this model, $\lambda(a)/\sigma(a) = 0.3264$.

Acknowledgments. This study was begun at the Institute of Geophysics and Planetary Physics, University of California, San Diego, and I am particularly indebted to F. Gilbert for his help and advice while I was there. I had several discussions with F. A. Dahlen and L. Cathles about the degree-1 Love numbers.

This work was partially supported by the Office of Naval Research.

REFERENCES

Alsop, L. E., and J. T. Kuo, The characteristic numbers of semi-diurnal earth tidal components for various earth models, *Ann. Geophys., 20,* 286, 1964.

Alterman, Z., H. Jarosch, and C. L. Pekeris, Oscillations of the earth, *Proc. Roy Soc. London, Ser. A, 252,* 80, 1959.

Alterman, Z., H. Jarosch, and C. L. Pekeris, Propagation of Rayleigh waves in the earth, *Geophys. J., 4,* 219, 1961.

Backus, G. E., Converting vector and tensor equations to scalar equations in spherical coordinates, *Geophys. J., 13,* 71, 1967.

Backus, G., and F. Gilbert, Uniqueness in the inversion of inaccurate gross earth data, *Phil. Trans. Roy. Soc. London, Ser. A, 266,* 123, 1970.

Ben-Menahem, A., S. J. Singh, and F. Solomon, Deformation of a homogeneous earth model by finite dislocations, *Rev. Geophys. Space Phys., 8,* 591, 1970.

Berger, J., and R. H. Lovberg, Earth strain measurements with a laser interferometer, *Science, 170,* 296, 1970.

Blum, P. A., and D. Hatzfeld, Étude régionale de l'influence océanique sur l'inclinaison: Premiers résultats à la station de Moulis, in *Sixth International Symposium on Earth Tides,* edited by R. Dejaiffe, p. 102, Royal Observatory of Belgium, Brussels, 1970.

Boussinesq, J., *Application des Potentiels à l'Étude de l'Équilibre et du Mouvement des Solides Élastiques,* 508 pp., Gauthier-Villars, Paris, 1885.

Caputo, M., Deformation of a layered earth by an axially symmetric surface mass distribution, *J. Geophys. Res., 66,* 1479, 1961.

Caputo, M., Tables for the deformation of an earth model by surface mass distributions, *J. Geophys. Res., 67,* 1611, 1962.

Cathles, L. M., The viscosity of the earth's mantle, Ph.D. thesis, Princeton Univ., Princeton, N.J., 1971.

Dahlquist, G., S. A. Gustafson, and K. Siklosi, Convergence acceleration from the point of view of linear programming, *Nord. Tidskr. Inform. Behandl., 5,* 1, 1965.

Darwin, G. H., Variations in the vertical due to elasticity of the earth's surface, in *Scientific Papers,* vol. 1, p. 430, Cambridge University Press, New York, 1907.

Farrell, W. E., Gravity tides, Ph.D. thesis, Univ. of Calif., San Diego, 1970.

Frazer, R. A., W. J. Duncan, and A. R. Collar, *Elementary Matrices,* 416 pp., Cambridge University Press, New York, 1965.

Gilbert, F., Excitation of the normal modes of the earth by earthquake sources, *Geophys. J., 22,* 223, 1970.

Gilbert, F., and G. E. Backus, Propagator matrices in elastic wave and vibration problems, *Geophysics, 31,* 326, 1966.

Gilbert, F., and G. Backus, Elastic-gravitational vibrations of a radially stratified sphere, in *Dynamics of Stratified Solids,* edited by George Herrmann, p. 82, American Society of Mechanical Engineers, New York, 1968*a*.

Gilbert, F., and G. Backus, A computational problem encountered in a study of the earth's normal modes, in *Proceedings of the Fall Joint Computer Conference,* p. 1273, Thompson, Washington, D.C., 1968*b*.

Gradshteyn, I. S., and I. M. Ryzhik, *Table of Integrals, Series, and Products,* 1086 pp., Academic, New York, 1965.

Harkrider, D. G., Surface waves in multilayered elastic media, 2, Higher mode spectra and spectral ratios from point sources in plane layered earth models, *Bull. Seismol. Soc. Amer., 60,* 1937, 1970.

Harrison, J. C., N. F. Ness, I. M. Longman, R. F. S. Forbes, E. A. Kraut, and L. B. Slichter, Earth tide observations made during the International Geophysical Year, *J. Geophys. Res., 68,* 1497, 1963.

Haubrich, R. A., The origin and characteristics of microseisms at frequencies below 140 cycles per hour, *Monographies de l'UGGI,* in press, 1972.

Hendershott, M., and W. Munk, Tides, *Annu. Rev. Fluid Mech., 2,* 205, 1970.

Hildebrand, F. B., *Introduction to Numerical Analysis,* 511 pp., McGraw-Hill, New York, 1956.

Hobson, E. W., *The Theory of Spherical and Ellipsoidal Harmonics,* 500 pp., Chelsea, New York, 1955.

Jeffreys, H., and R. O. Vicente, The theory of nutation and the variation of latitude, *Mon. Notic. Roy. Astron. Soc., 117,* 142, 1957.

Jobert, G., Perturbations des marées terrestres, *Ann. Geophys., 16,* 1, 1960.

Kaula, W. M., Elastic models of the mantle corresponding to variations in the external gravity field, *J. Geophys. Res., 68,* 4967, 1963.

Kuo, J. T., Static response of a multilayered medium under inclined surface loads, *J. Geophys. Res., 74,* 3195, 1969.

Kuo, J. T., R. C. Jachens, M. Ewing, and G. White, Transcontinental tidal gravity profile across the United States, *Science, 168,* 968, 1970.

Lagus, P. L., and D. L. Anderson, Tidal dissipation in the earth and planets, *Phys. Earth Planet. Interiors, 1,* 505, 1968.

Lamb, H., On Boussinesq's problem, *Proc. London Math. Soc., 34,* 276, 1902.

Lamb, H., On the deflection of the vertical by tidal loading of the earth's surface, *Proc. Roy. Soc. London, Ser. A, 93,* 293, 1917.

Lambert, A., The response of the earth to loading by the ocean tides around Nova Scotia, *Geophys. J., 19,* 449, 1970.

Longman, I. M., A Green's function for determining the deformation of the earth under surface mass loads, 1, Theory, *J. Geophys. Res., 67,* 845, 1962.

Longman, I. M., A Green's function for determining the deformation of the earth under surface mass loads, 2, Computations and numerical results, *J. Geophys. Res., 68,* 485, 1963.

Love, A. E. H., The stress produced in a semi-infinite solid by pressure on part of the boundary, *Phil. Trans. Roy. Soc. London, Ser. A, 228,* 377, 1929.

McConnell, R. K., Isostatic adjustment in a layered earth, *J. Geophys. Res., 70,* 5171, 1965.

Molodensky, M. S., The theory of nutation and diurnal earth tides, in *Fourth International Symposium on Earth Tides,* edited by P. Melchior, p. 25, Royal Observatory of Belgium, Brussels, 1961.

Munk, W. H., and G. J. F. MacDonald, *The Rotation of the Earth,* 323 pp., Cambridge University Press, New York, 1960.

Munk, W., F. Snodgrass, and M. Wimbush, Tides off-shore: Transition from California coastal to deep-sea waters, *Geophys. Fluid Dyn., 1,* 161, 1970.

National Physical Laboratory, *Modern Computing Methods,* 170 pp., Philosophical Library, New York, 1961.

Pekeris, C. L., and Y. Accad, Solution of Laplace's equations for the M_2 tide in the world oceans, *Phil. Trans. Roy. Soc. London, Ser. A, 265,* 413, 1970.

Pekeris, C. L., and H. Jarosch, The free oscillations of the earth, in *Contributions in Geophysics in Honor of Beno Gutenberg,* vol. 1, edited by H. Benioff, M. Ewing, B. Howell, and F. Press, p. 171, Pergamon, New York, 1958.

Pertsev, B. P., On the effect of ocean tides on tidal variations of gravity, *Izv. Acad. Sci. USSR Phys. Solid Earth, 10,* 25, 1966.

Pertsev, B. P., The effect of ocean tides upon earth-tide observations, in *Sixth International Symposium on Earth Tides,* edited by R. Dejaiffe, p. 113, Royal Observatory of Belgium, Brussels, 1970.

Prothero, W. A., and J. M. Goodkind, Earth-tide measurements with the superconducting gravimeter, *J. Geophys. Res., 77,* 926, 1972.

Rayleigh, Lord (J. W. Strutt), *The Theory of Sound,* vol. 1, 480 pp., Dover, New York, 1945.

Shanks, E. B., Solutions of differential equations by evaluations of functions, *Math Comput., 20,* 21, 1966.

Singh, S. J., Static deformation of a multilayered half-space by internal sources, *J. Geophys. Res., 75,* 3257, 1970.

Singh, S. J., and A. Ben-Menahem, On the summation of certain Legendre series, *J. Eng. Math., 2,* 275, 1968.

Slichter, L. B., and M. Caputo, Deformation of an earth model by surface pressures, *J. Geophys. Res., 65,* 4151, 1960.

Snodgrass, F. E., Deep sea instrument capsule, *Science, 162,* 78, 1968.

Stoneley, R., The elastic yielding of the earth, *Mon. Notic. Roy. Astron. Soc. Geophys., Suppl., 1,* 356, 1926.

Takeuchi, H., On the earth tide of the compressible earth of variable density and elasticity, *Eos Trans. AGU, 31,* 651, 1950.

Takeuchi, H., M. Saito, and N. Kobayashi, Statical deformations and free oscillations of a model earth, *J. Geophys. Res., 67,* 1141, 1962.

Terazawa, K., On periodic disturbance of level arising from the load of neighboring oceanic tides, *Phil. Trans. Roy. Soc. London, Ser. A, 217,* 35, 1916.

Watson, G. N., *A Treatise on the Theory of Bessel Functions,* 804 pp., Cambridge University Press, New York, 1966.

Wiggins, R. A., Terrestrial variational tables for the periods and attenuation of the free oscillations, *Phys. Earth Planet. Interiors, 1,* 201, 1968.

Zienkiewicz, O. C., *The Finite Element Method in Engineering Science,* 521 pp., McGraw-Hill, New York, 1971.

(Received November 23, 1971; revised March 20, 1972.)